

**COMPARATIVE ANALYSIS OF HEAT TRANSFER
THROUGH TRIANGULAR FIN USING NUMERICAL
TECHNIQUES AND ANSYS**

*Submitted in partial fulfilment of the requirement for the award of the degree
of*

MASTER OF TECHNOLOGY

(MECHANICAL ENGINEERING)

TO

DELHI TECHNOLOGICAL UNIVERSITY



SUBMITTED BY

ANUJ ARYA

ROLL NO.- 2K16/THE/05

(UNDER THE SUPERVISION OF)

N.A. ANSARI

ASSISTANT PROFESSOR

**DEPARTMENT OF MECHANICAL, PRODUCTION & INDUSTRIAL
AND AUTOMOBILE ENGINEERING
DELHI TECHNOLOGICAL UNIVERSITY**

BAWANA ROAD, DELHI- 110042

JULY, 2018

CANDIDATE’S DECLARATION

I, Anuj Arya, 2K16/THE/05, Student of M.Tech (THERMAL ENGINEERING), hereby declare that this project titled “COMPARATIVE ANALYSIS OF HEAT TRANSFER THROUGH TRIANGULAR FIN USING NUMERICAL TECHNIQUES AND ANSYS” which is submitted by me to the Department of Mechanical Engineering, Delhi Technological University, Delhi in partial fulfillment of the requirement for the award of the degree of Master of Technology, is my own work and that, to the best of my knowledge and belief, it contains no material previously published or written by another person nor material which to a substantial extent has been accepted for the award of any other degree or diploma of the university or other institute of higher learning, except where due acknowledgment has been made in the text.

Place: Delhi
Date:

ANUJ ARYA (2K16/THE/05)

CERTIFICATE

This is to certify that the dissertation work entitled “**Comparative Analysis Of Heat Transfer Through Triangular Fin Using Numerical Techniques And Ansys**” which is submitted by Anuj Arya, 2K16/THE/05 [Mechanical Engineering], Delhi Technological University, Delhi in partial fulfillment of the requirement for the award of the the degree of Master of Technology, is a record of the project work carried out by the student under my supervision.

Place: Delhi

Date:

(Signature Of Supervisor)

ASST. PROF. N.A. ANSARI

ACKNOWLEDGEMENT

We would like to acknowledge with appreciation the numerous and valuable guidance, comments and suggestions for this work.

We express our gratitude to **Asst. Prof. N.A. Ansari, Department of Mechanical Engineering**, who, inspite of his busy schedule, provided guidance, motivation, help and support for the successful completion of the present project work. His role in the successful completion of the project up to the stage was highly appreciable and valuable.

We wish to sincerely thank **the Head, Mechanical, Production & Industrial And Automobile Engineering Department, Prof. Vipin**, for his extended support and help in carrying out this project work.

Also, we would like to thank my project colleagues and my Mechanical Engineering friends for their help and suggestions in the successful completion of the project work.

Thank you

ABSTRACT

The current project work problem has been proposed and its purpose is to investigate the detailed parameters of the conjugate convection of the surface radiation of a typical non-uniform fin, triangular fin. The equation of control of the temperature distribution along the fins is obtained by appropriate conduction, energy balance between convection and radiant heat. The resulting nonlinear differential equations are converted to algebraic form by appropriate finite difference formulas. Solving the algebraic equations obtained using the Gauss-Seidel iterative solver.

Computer code in C++ is specifically designed to solve this problem. Grid sensitivity analysis has been performed to achieve the best grid scale. In the above exercises, unequally spaced and equally spaced grids were tried. Discussed in detail the independent parameters, namely the thermal conductivity of the fin material, the surface emissivity and the effect of the convection heat transfer coefficient on the local fin temperature distribution.

Keywords: *Non-uniform triangular fin, Conjugate Convection, Surface Radiation, Finite Difference Method.*

TABLE OF CONTENTS

| | |
|--|------|
| DECLARATION | i |
| CERTIFICATE | ii |
| ACKNOWLEDGEMENT | iii |
| ABSTRACT | iv |
| TABLE OF CONTENTS | v |
| LIST OF FIGURES | vii |
| LIST OF GRAPHS | viii |
| NOMENCLATURE | x |
| Greek Symbols:..... | x |
| SUBSCRIPTS | xi |
| 1. INTRODUCTION..... | 1 |
| 1.1 Literature Review | 1 |
| 1.2 Broad Objective of the Work..... | 5 |
| 2. PROBLEM DEFINITION AND MATHEMATICAL FORMULATION..... | 6 |
| 2.1 Assumptions in deriving the governing equations and energy balance..... | 8 |
| 2.2 Calculation of surface area and cross-sectional area | 13 |
| 2.2.2 For the tip | 15 |
| b. To Calculate Cross-sectional Area | 15 |
| 3. METHOD OF SOLUTION AND RANGE OF PARAMETERS.... | 17 |
| 3.1 Discretization of the governing equations for uniform grids | 17 |
| 3.1.1 At the base of the fin | 17 |
| 3.1.2 For the interior nodes | 18 |
| 3.1.3 For the Tip | 19 |
| 3.2 Discretization of the governing equations for non-uniform grids | 20 |
| 3.3 Solution Methodology to algebraic equations | 20 |
| 3.4 Range of parameter..... | 21 |
| 4. Observation through Ansys..... | 21 |

| | |
|--|----|
| 4.1 Variation of temperature along length of fin for varying emissivity at $T_b=400C$ | 21 |
| 4.2 Variation of temperature along length of fin for varying emissivity at $T_b= 500C$ | 23 |
| 4.3 Variation of temperature along length of fin for varying convective coefficient at $T_b= 400C$ | 24 |
| 4.4- Variation of temperature along the length of fin for varying convective coefficient , when $\epsilon=0.25$, $T_b= 500^\circ C$, $h= 5w/m^2^\circ c$ | 25 |
| 4.5- Variation of temperature along the length fin for varying emissivity at $k=1w/m^\circ c$, $T_b= 400^\circ C$ & $h= 5w/m^2^\circ C$ | 27 |
| 5. Result & Discussion | 29 |
| 5.1 Grid Sensitivity Test | 29 |
| 5.2 Comparison between ansys result & c++ result | 32 |
| 5.2.1 When $T_b=400C$, $K=205W/MC$, $h= 5 w/m^2c$ | 32 |
| 5.2.2 When $T_b=500C$, $k= 205w/mc$, $h=5w/m^2C$, | 33 |
| 5.2.3 When $T_b = 400C$, $k = 205w/mc$, varying h at emissivity= $0.25\&.75$ | 34 |
| 5.2.4 When $T_b = 500C$, $k=205w/mc$, varying h , at emissivity = $0.25\&0.75$ | 35 |
| 5.2.5 When $T_b=400C$, $k=1w/mc$, $h= 5w/m^2c$ & varying emissivity at $0.25\&0.75$ | 37 |
| 6. Concluding Remarks & Scope For Future Work | 39 |
| 6.1 Scope For Future Work..... | 40 |
| References | 41 |

LIST OF FIGURES

| | |
|--|-----------|
| Figure 1: Schematic of triangular fin geometry..... | 6 |
| Figure 2: Uniform grid system used to discretize the computational domain..... | 7 |
| Figure 3: Energy balance for the mth node(semi- element)..... | 9 |
| Figure 4: Energy balance for the interior element..... | 10 |
| Figure 5: Energy balance for the tip..... | 12 |
| Figure 6: Calculation of surface area and cross sectional area..... | 14 |
| <i>Figure 7: Emissivity = 0.25</i> | <i>22</i> |
| <i>Figure 8: Emissivity = 0.75</i> | <i>23</i> |
| <i>Figure 9: Convection heat transfer coefficient = 5 w/m² C</i> | <i>23</i> |
| <i>Figure 10: Convection heat transfer coefficient = 50 W/m² C.....</i> | <i>24</i> |
| <i>Figure 11: Thermal Conductivity = 205 W/m C.....</i> | <i>26</i> |
| <i>Figure 12: Thermal conductivity = 0.1 W/m C</i> | <i>26</i> |

LIST OF GRAPHS

| | |
|---|----|
| <i>Graph 1: Local Temperature distribution along the Length of the fin for $\epsilon=0.25$ at $T_b=400^\circ\text{C}$, $K=205\text{w/mc}$ & $h= 5\text{w/m}^2\text{C}$.....</i> | 21 |
| <i>Graph 2: Local Temperature distribution along the Length of the fin for $\epsilon=0.5$ at $T_b=400^\circ\text{C}$, $K=205\text{w/mc}$ & $h= 5\text{w/m}^2\text{C}$.....</i> | 22 |
| <i>Graph 3: Local Temperature distribution along the Length of the fin for $\epsilon=0.75$ at $T_b=400^\circ\text{C}$, $K=205\text{w/mc}$ & $h= 5\text{w/m}^2\text{C}$.....</i> | 22 |
| <i>Graph 4: Local Temperature distribution along the Length of the fin for for $\epsilon=0.25$ at $T_b=500^\circ\text{C}$, $K=205\text{w/mc}$ & $h= 5\text{w/m}^2\text{C}$.....</i> | 23 |
| <i>Graph 5: 3 Local Temperature distribution along the Length of the fin for for $\epsilon=0.25$ at $T_b=500^\circ\text{C}$, $K=205\text{w/mc}$ & $h= 5\text{w/m}^2\text{C}$.....</i> | 23 |
| <i>Graph 6: 3 Local Temperature distribution along the Length of the fin for for $\epsilon=0.25$ at $T_b=500^\circ\text{C}$, $K=205\text{w/mc}$ & $h= 5\text{w/m}^2\text{C}$.....</i> | 24 |
| <i>Graph 7: Local Temperature Distribution along the fin for $h=5\text{w/m}^2\text{c}$, $T_b= 400^\circ\text{C}$ & $K=205\text{w/m}^\circ\text{c}$.....</i> | 24 |
| <i>Graph 8: Local Temperature Distribution along the fin for $h=10\text{w/m}^2\text{c}$, $T_b= 400^\circ\text{C}$ & $K=205\text{w/m}^\circ\text{c}$.....</i> | 25 |
| <i>Graph 9: Local Temperature Distribution along the fin for $h=15\text{w/m}^2\text{c}$, $T_b= 400^\circ\text{C}$ & $K=205\text{w/m}^\circ\text{c}$.....</i> | 25 |
| <i>Graph 10: Local Temperature Distribution along the fin for $h=5\text{w/m}^2\text{c}$, $T_b= 500^\circ\text{C}$ & $K=205\text{w/m}^\circ\text{c}$.....</i> | 26 |
| <i>Graph 11: 5 Local Temperature Distribution along the fin for $h=10\text{w/m}^2\text{c}$, $T_b= 500^\circ\text{C}$ & $K=205\text{w/m}^\circ\text{c}$.....</i> | 26 |
| <i>Graph 12: 5 Local Temperature Distribution along the for $h=15\text{w/m}^2\text{c}$, $T_b= 500^\circ\text{C}$ & $K=205\text{w/m}^\circ\text{c}$.....</i> | 27 |
| <i>Graph 13: Local Temperature Distribution along the fin for $k=1\text{w/m}^\circ\text{c}$, $T_b= 400^\circ\text{C}$ & $h= 5\text{w/m}^2\text{c}$ at $\epsilon= 0.25$.....</i> | 27 |
| <i>Graph 14: Local Temperature Distribution along the fin for $k=1\text{w/m}^\circ\text{c}$, $T_b= 400^\circ\text{C}$ & $h= 5\text{w/m}^2\text{c}$ at $\epsilon= 0.5$.....</i> | 28 |

Graph 15: Local Temperature Distribution along the fin for $k=1w/m^{\circ}c$, $T_b=400^{\circ}C$ & $h= 5w/m2^{\circ}c$ at $\epsilon= 0.75$28

Graph 16: When Base Temperature is $400^{\circ}C$, $k=205w/mC$ and $h= 5w/m2C$. When Emissivity(ϵ)= 0.25.....32

Graph 17: When Base Temperature is $400^{\circ}C$, $k=205w/mC$ and $h= 5w/m2C$. When Emissivity(ϵ)= 0.75.....32

Graph 18: When Base Temperature $T_b= 500^{\circ}C$, $K= 205W/m^{\circ}c$ & $h= 5W/m2^{\circ}c$. Emissivity= 0.25.....33

Graph 19: When Base Temperature $T_b= 500^{\circ}C$, $K= 205W/m^{\circ}c$ & $h= 5W/m2^{\circ}c$. Emissivity= 0.75.....34

Graph 20: When Base Temperature $T_b= 400$, $K= 205W/m^{\circ}C$, $h= W/m2^{\circ}C$ & Emissivity (ϵ)= 0.25 When $h= 5W/m2^{\circ}C$34

Graph 21: When Base Temperature $T_b= 400$, $K= 205W/m^{\circ}C$, $h= W/m2^{\circ}C$ & Emissivity (ϵ)= 0.25 When $h= 50W/m2^{\circ}C$35

Graph 22: When Base Temperature $T_b= 500^{\circ}C$, $K= 205W/m^{\circ}C$, Emissivity(ϵ)= 0.75. When $h= 5W/m2^{\circ}C$35

Graph 23: When Base Temperature $T_b= 500^{\circ}C$, $K= 205W/m^{\circ}C$, Emissivity(ϵ)= 0.75. When $h= 50W/m2^{\circ}C$36

Graph 24: Base Temperature $T_b= 400^{\circ}C$, $K= 1W/m^{\circ}C$, $h= 5W/m2^{\circ}C$. When Emissivity (ϵ) = 0.25.....36

Graph 25: Base Temperature $T_b= 400^{\circ}C$, $K= 1W/m^{\circ}C$, $h= 5W/m2^{\circ}C$. When Emissivity (ϵ) = 0.75.....37

NOMENCLATURE

A – Cross sectional area (in m^2)

AR – Aspect Ratio = L/t .

h - Convective heat transfer coefficient in $W/m^2 C$.

k - Thermal conductivity of the fin material in $W/m C$.

L – Protruding Length of the geometry in, m.

n – Number of nodes in the direction of heat transfer.

S - Surface area in, m^2 .

T_a - Ambient Temperature in, C.

x – Elemental thickness in Cartesian system in, m

T_b – Base or Primary surface temperature of the fin in $^{\circ}C$ or K

w – Width of the fin in m.

Greek Symbols:

β - Semi angle in degrees.

ϵ – Surface Emissivity

σ - Stefan-Boltzmann Constant = $5.6697 \times 10^{-8} W/m^2 K^4$

Θ – Local temperature excess in $^{\circ}C$ or K = $T(x) - T_a$

SUBSCRIPTS

| | |
|-------------------|--|
| a | Ambient condition |
| b | Conditions at the base of the fin |
| i | Number of nodes in r (or) x direction. |
| M | m th node in the direction of heat transfer. |
| <i>q Cond in</i> | Heat conducted into an element, W. |
| <i>q cond out</i> | Heat conducted out from an element, W |
| <i>q conv</i> | Heat convected out, W. |
| <i>qrad</i> | Heat radiated, W. |
| cond, x, in | conduction heat transfer into an element along the fin |
| cond, x, out | conduction heat transfer out of an element along the fin |
| conv | Convection heat transfer from an element |
| rad | Heat transfer by surface radiation from an element |
| <i>i</i> | Any arbitrary element along the fin |

1. INTRODUCTION

1.1 Literature Review

Since current project work involves the numerical study of a class of fin geometries using air as the cooling medium, a comprehensive review of the literature relating to multimode heat transfer is made, especially the same literature as fins. The same summary will be provided below.

Sandhya Mirapalli and P.S. Kishore [1], In this paper heat transfer analysis is done by placing rectangular and triangular fins. The analysis was carried out from 200oC to 600oC by varying the temperature of the cylinder surface, ranging from 6 cm to 14 cm. Input parameters such as input density, heat transfer coefficient, thermal conductivity and fin thickness determine the output parameters such as heat flow rate, heat flux per unit mass, efficiency and effect. Comparison with rectangular fins. M. Sudheer [2], In the paper, detailed work has been carried out to develop a finite element method to estimate the temperature distribution of steady-state heat transfer and thermal stress caused by temperature differences in silicon carbide (SiC) ceramic finned tubes. Transfer device. The results obtained are shown in a series of temperature and thermal stress distribution curves. The annular fins have a rectangular, trapezoidal and triangular profile and are suitable for various radius ratios. The results show that the radius ratio and fin profile are important parameters affecting the temperature and thermal stress distribution of the annular fin, using Ansys. G.C. Rao [3], This paper presents a simulation study of surface radiation from conjugated convection, which is derived from a movable open cavity that is nested in a discrete heat source mounted on the left wall. G.C. Rao and Other [4], Numerical results of surface radiation of conjugate convection and four discrete heat sources mounted on the right side of a finite thickness vertical channel wall have been proposed. Based on numerical studies, the flow and heat transfer

characteristics are derived by varying the parameters Re_S , Gr_S , ep , es , $k_p = k_f$ and $k_s = k_f$ over a wide range. Zinnes [5],

After study paper the main objective is to detected a stable natural convection distribution of two-dimensional laminar flow from a thermally conductive vertical plate of finite thickness with any surface heat. Obviously, only two heat transfer modes (conduction and free convection) are involved here. Zinnes reports the temperature, velocity and temperature distribution characteristics of the plate in the boundary layer of the plate by considering the thermal properties of the plate along the plate and the thermal distribution of the plate as independent parameters. Zinnes validated his numerical results with some of his experimental results. The main corollary of his work is that the degree of coupling between conduction and free convection is significantly affected by the ratio of the thermal conductivity of the plate to the fluid. Dharma Rao and others [6], Numerically solved the problem of laminar natural convection heat transfer in fin array. They consider a vertical pedestal with horizontal fins and solve the heat conduction equations in the energy control equation and fins They validated their numerical results using experimental data obtained from the literature, and discussed the effects of parameters such as parameter temperature, fin height and fin spacing on heat transfer rate of fin arrays. A.A. Dahghan [7], Natural convection, conduction and radiant heat transfer combined in an open top upright chamber containing discrete heat sources have been digitally modeled . The surface emissivity has changed, and the effects on the flow field and the thermal field have been determined for different Rayleigh values, and the comparison of numerical results with experimental observations shows that the accurate prediction of the flow field and the thermal field depends largely on Radiative heat transfer in the case of logarithmic values. S. Abrate [8], Use the finite element method to model when conducting in an array of triangular fins with attached walls. Developed an adaptive mesh refinement technique that provides accuracy comparable to uniform mesh refinement and greatly increases computational efficiency. For various Biot numbers, check the effect of wall thickness and fin spacing. Jing Ma [10], Spectral Element Method (SEM) was developed to address coupled conduction, convection and radiative heat transfer in

moving trapezoidal, convex parabolic and concave parabolic porous fins. In these irregular porous fins, uneven heat generation, heat transfer coefficient and surface emissivity vary with temperature, M.P. Shah [13], In this paper, the Ansys APDL software was used to numerically study copper, AA1100, AA2011, AA3105 and other materials. Transient and steady-state analysis of cylindrical fins under convection and specified base temperature conditions. Specify the length of the fin, the thickness of the base and the thickness of the end. Specify the thermal conductivity of the fin material. R.S.K. Reddy and other [14], The purpose of this paper is to examine the effect of the fin shape of the heat sink on thermal performance. Various types of perforations on pin fins for efficient heat transfer under constant heat flux conditions. Performing 3D modeling and analysis using CATIA and ANSYS by using forced convection of the fan to complete numerical simulation, 12.0. This will help identify new fin topologies with better heat transfer characteristics than traditional planar fins. The main goal is to increase the rate of heat transfer through the fin surface and reduce the material cost. S.H. Barhatte [15], In this paper, the fin plane was modified by cutting the notch to remove the central fin portion. This article presents an experimental analysis of the results obtained over a range of fin heights and heat dissipation rates. Try to compare the experimental results with those obtained using CFD software. R. Gupta and Others [16], Objective of the paper is to implementation is to increase the heat dissipation rate by using an invisible working fluid, only the air. We know that by increasing the surface area, the heat dissipation rate can be increased, so it is very difficult to design such a large complex engine. The main purpose of using these heat sinks is to cool the engine cylinders with air. The main purpose of the project is to analyze thermal properties by changing the geometry of the cylindrical fin material. M. Jain [17], The main purpose of the paper is to analyze the heat dissipation of the fins by changing the geometry of the fins. Parametric model of fins has been developed to predict transient thermal behavior. Later, the model is created by changing the geometry, such as rectangles, circles, triangles, and fins with extensions. The modeling software used is CREO Parametric 2.0. Analyze using ANSYS 14.5. The material currently used to make fins is usually aluminum alloy 204, which has a

thermal conductivity of 110-150 W / m- ° C. We are using aluminum alloy 6061 material to analyze the fins, aluminum alloy 6061 has a higher thermal conductivity, about 160-170W / m-0C. After the material is determined, the third step is to increase the heat transfer rate of the system by changing geometric parameters such as cross-sectional area, parameters, length, thickness, and the like. Eventually led us to form fins of different shapes and geometries. A. Aziz [19], The purpose of the work in this paper is to two fold. The first objective is to obtain a finite element solution for a two-dimensional triangular fin and to provide heat transfer data for a wide range of Biot numbers and length to substrate thickness so that the information can be used for prediction and design purposes. The second purpose is to report additional data for the rectangular fins to complement the results of Lau and Tan. D.C. Look [25], Paper conclude that, when the coordinates and system geometry are not collinear, the solution to the variable separation method is not an exact solution. There is a region where there is a clear and accurate solution. For the case given here, when R is large (ie, when the length) In fact, for the limited range of parameters used here, the error in the root temperature is very small for R small (ie R<0.1). So while this limitation is cumbersome, it is a problem that a wing designer might be able to solve. The h of the fins becomes smaller - the protrusions on the surface) and the solution has obvious errors at the root.

Looking at the literature, a brief summary has been provided here, revealing that the interaction of surface radiation with fin conjugate convection over non-uniform cross-sections and surface areas has not been discussed in detail. Therefore, current project work aims to perform a comprehensive numerical simulation of the multi-mode heat transfer of triangular fins.

1.2(a) Research Gap

Heat transfer analysis of a triangular fin done with analytical method, numerical techniques, experimentally by using of thermocouple and also done with used of ansys software, my project work research gap is to show the difference of results which get from numerical technigue and ansys for same input parameters in terms of temperature distribution along the length of fin.

1.2(b) Broad Objective of the Work

As mentioned above, the fin geometry of the non-uniform cross-section, ie triangular fins, will be used for the study. The relevant control equations for the temperature distribution will be derived to use energy balance to solve all the heat transfer modes involved in the problem.

The resulting differential equations (ordinary differential equations) for the entire computational domain will be converted to algebraic forms using the finite difference method. Solving algebraic equations so obtained using Gauss-Seidel iterative techniques.

Heat transfer analysis on triangular fin geometries of the same size is also done with the help of the ansys software, which represents changing the temperature over the length of the cross section. Observe changes in temperature according to various physical parameters, such as emissivity, thermal conductivity, convection heat transfer coefficient, etc. compare the result obtained from C++ with the result of Ansys software. Variations in the temperature distribution over the geometric length of the triangular fin are plotted on the graphs.

2. PROBLEM DEFINITION AND MATHEMATICAL FORMULATION

Figure 1 shows a schematic of the geometry of the problem considered for the study in the current project work. It contains of fins with non- uniform cross section area of a triangular geometry. The fin protrudes from the base surface up to a length L and the base thickness is t . When the thickness is moved along the protruding length or heat transfer direction, the thickness decreases linearly and reaches the point at the tip of the fin. Assume that the bottom or bottom of the fin is insulated and maintained at temperature T_b .

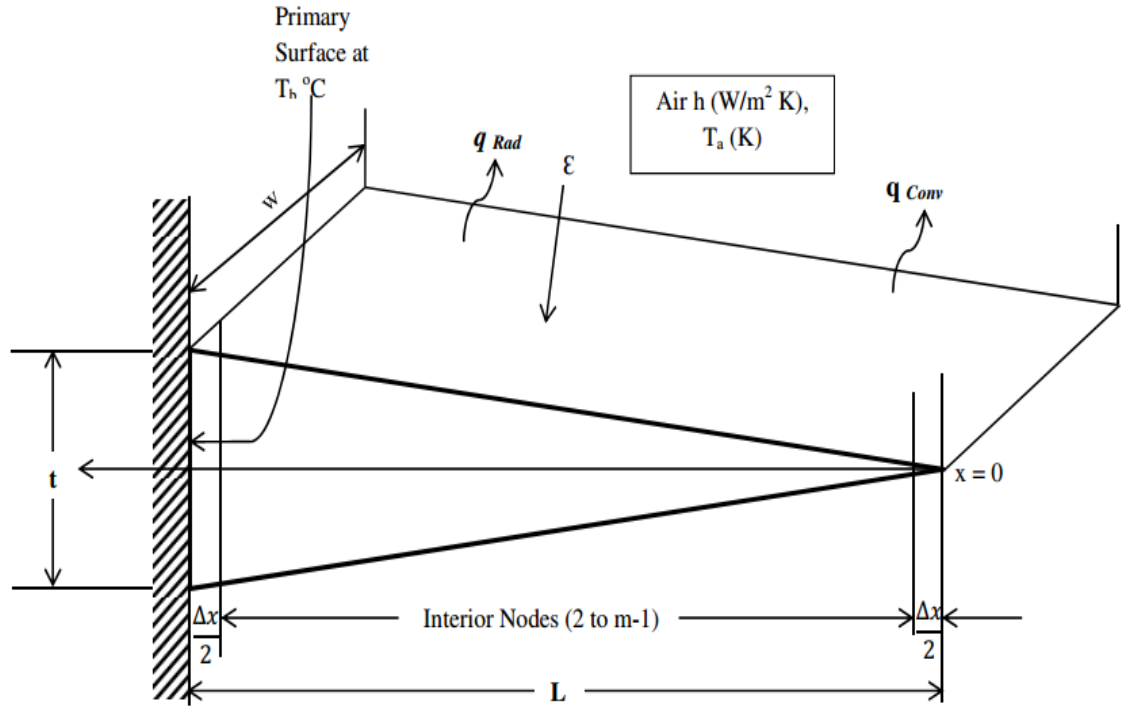


Figure 1: Schematic of Triangular Fin Geometry

The heat conduction through the fins is one-dimensional, stable, and there is no internal heat generation inside the fins. The heat sink material has a thermal conductivity of k and surface emissivity. The heat conducted on the fin base surface penetrates or conducts along the length of the fins and then dissipates from the top and bottom side surfaces by a combined pattern of convection and radiation.

The air that is considered to be transparent to radiation is a cooling medium. Assume that the temperature is T_a and the convection heat transfer coefficient is h . From the above, it can be understood that since the current project work problem involves the use of digital solutions, it is proposed to write computer code for solving the problem.

2.1 Deducing the assumptions of the control equation and energy balance

- a. One-dimensional steady state heat conduction .
- b. Bay ambient heat dissipation can only be done through the side.
- c. Assume that the main surface of the fin is at a constant temperature T_b .

By using the above assumptions, the energy equation is derived for discrete nodes in the computing domain .Figure 2 shows the field of computation for current project work issues . The heat conducted at the bottom of the fins is eventually dissipated by the side surfaces of the fins by the combined pattern of convection and radiation.

Assuming that the major surfaces of the fins are maintained at Dirichlet boundary conditions (eg, melting of solids or boiling of liquids), the internal nodes and tips undergo conjugate (convection and radiation) boundary conditions.

A typical energy balance:

2.2.1 At the base ($i = m$)

The semi-element is shown in Figure 3. At the bottom of the fin of the m th node at $x = L$, the Dirichlet or thermostatic boundary conditions yield the following equation.

$$T(m) = T_b \dots\dots\dots 2.1$$

$$\theta = T_b - T_a \dots\dots\dots 2.2$$

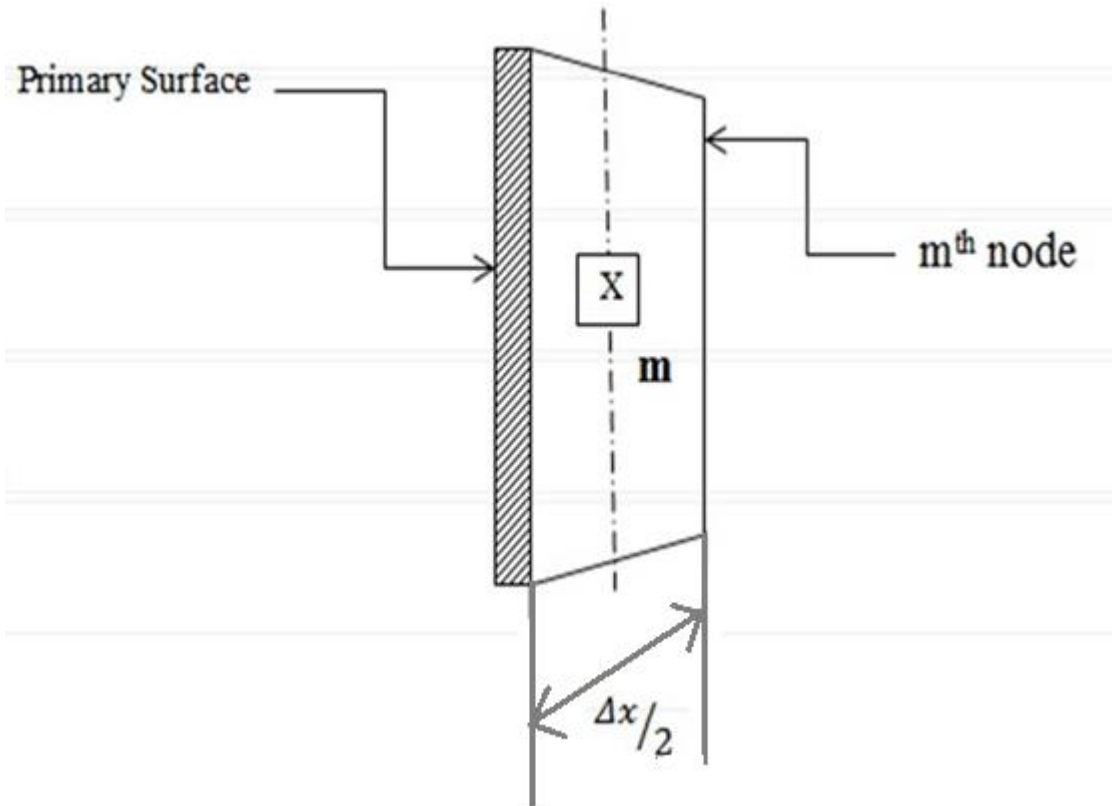


Figure 2: Energy Balance for mth node (semi element)

2.1.2 For the interior Nodes ($i = 2$ to $m - 1$)

Heat transferred into any intermediate element by conduction exits the element by convection and radiation, and a portion thereof conducts to the next element. Figure 4 shows a schematic of an internal component. The energy balance of any element of the internal node applies to all internal elements. Suppose the two surfaces dissipate the same amount of heat, where the surface area is taken twice to account for convection and radiation from both sides.

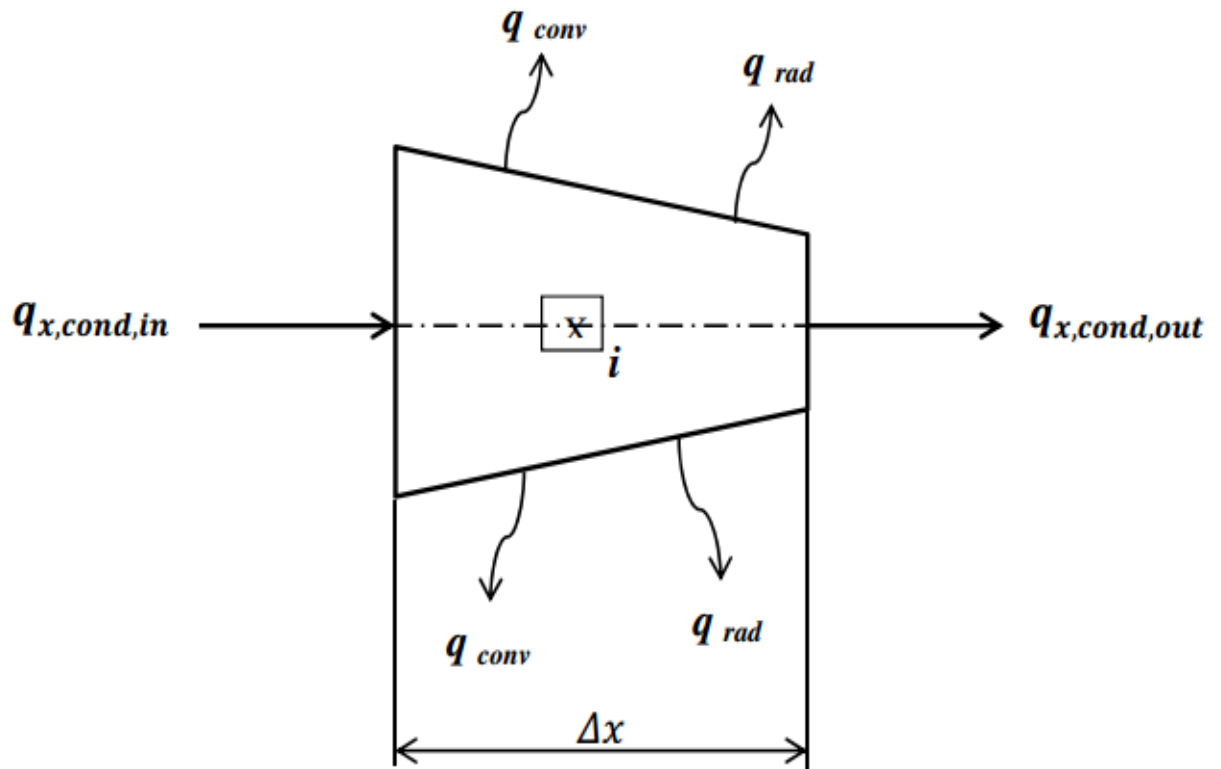


Figure 3: Energy balance for the interior element

The energy balance for an element is given by:

$$(Q_{\text{cond.}})_{\text{in}} = (Q_{\text{cond.}})_{\text{out}} + (Q_{\text{conv.}}) + (Q_{\text{rad.}}) \dots \dots \dots 2.3$$

By Using of Taylor Series,

$$q_{x+dx} = q_x + \frac{\partial(q_x)}{\partial x} \Delta x * \frac{1}{1!} + \dots \dots \dots + \text{tranding}$$

$$Q_x = Q_x + \frac{\partial}{\partial x}(Q_x) dx + (Q_{\text{cov.}}) + (Q_{\text{rad.}})$$

$$\text{Or, } \frac{\partial}{\partial x}(Q_x)dx + (Q_{\text{conv.}}) + (Q_{\text{rad.}}) = 0$$

$$\text{Or, } \frac{\partial}{\partial x}(-kA \frac{d\theta}{dx}) dx + hPdx(T_i - T_a) + \sigma \epsilon ds(T_i^4 - T_a^4) = 0$$

$$\text{Or, } \frac{\partial}{\partial x}(-kA \frac{d\theta}{dx}) dx + hds\theta + \sigma \epsilon ds(T_i^4 - T_a^4) = 0$$

$$\text{Where } A = \left(\frac{t*x}{L}\right)w$$

$$\text{or, } -k \left[\frac{\partial}{\partial x} \left(\frac{t*x*w}{L} \right) \frac{d\theta}{dx} \right] + h \frac{ds}{dx} \theta + \sigma \epsilon \frac{ds}{dx} (T_i^4 - T_a^4) = 0$$

$$- \frac{k*t*w}{L} \left[\frac{d\theta}{dx} + x * \frac{d^2\theta}{dx^2} \right] + h \frac{ds}{dx} \theta + \sigma \epsilon \frac{ds}{dx} (T_i^4 - T_a^4) = 0$$

$$\text{Or, } -k \left(\frac{t*x*w}{L} \right) \frac{d^2\theta}{dx^2} - k \left(\frac{t*w}{L} \right) \frac{\Delta x}{\Delta x} \frac{d\theta}{dx} + h \frac{ds}{dx} \theta + \sigma \epsilon \frac{ds}{dx} (T_i^4 - T_a^4) = 0$$

$$-kA \left(\frac{d^2\theta}{dx^2} \right) - k \left(\frac{dA}{dx} \right) \left(\frac{d\theta}{dx} \right) + h \left(\frac{ds}{dx} \right) \theta + \sigma \epsilon \frac{ds}{dx} (T_i^4 - T_a^4) = 0$$

In the above equation (2.3) is expanded using Taylor's series expansion. Now, appropriate equations are substituted in the place of each term and simplified, which results in the following:

$$\left(\frac{d^2\theta}{dx^2} \right) + \frac{1}{A} \left(\frac{dA}{dx} \right) \left(\frac{d\theta}{dx} \right) - \frac{h}{kA} \left(\frac{ds}{dx} \right) \theta - \frac{\sigma \epsilon}{kA} \frac{ds}{dx} (T_i^4 - T_a^4) = 0 \dots\dots 2.4$$

2.2.3 At the tip (i = 1)

The fin tip is a half element. The tip of the fin is considered to convection and radiate heat to the environment, as shown in Figure 5. The resulting energy balance leads to the following equation. The surface area is also double here, assuming that the two surfaces are dissipated into the environment by combining equal amounts of convection and radiation.

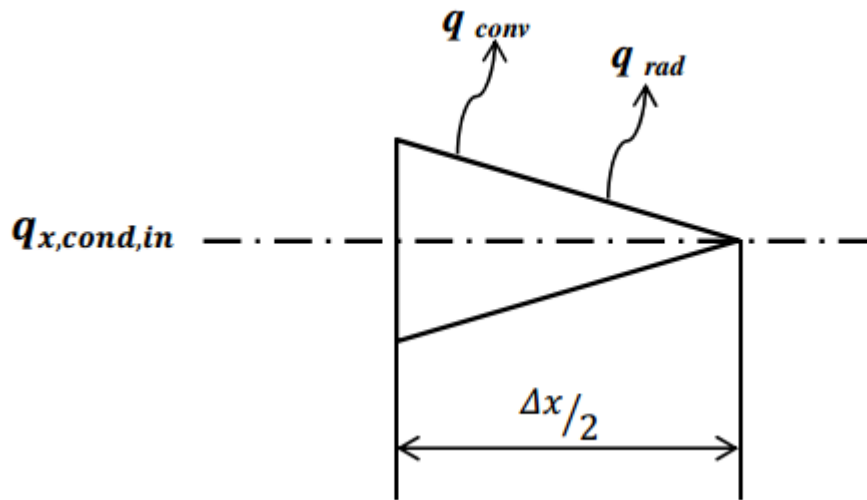


Figure 4: Energy Balance for the tip

Energy balance is given by,

$$-Q_{x \text{ cond. in}} = Q_{\text{conv.}} + Q_{\text{rad.}} \dots\dots\dots(2.5)$$

Here the conduction term is considered to be negative because initially we have assumed the right-to-left heat transfer direction (x direction) . But in actual case it is from base to tip of the fin i.e. left to right.

$$\text{Or,} \quad -Q_x = h(PdA)\theta + \sigma \epsilon dS(T_i^4 - T_a^4)$$

$$\text{Or,} \quad -(-kA \frac{d\theta}{dx}) = hds\theta + \sigma \epsilon ds(T_i^4 - T_a^4)$$

$$\text{Or,} \quad -kA \frac{d\theta}{dx} + hds\theta + \sigma \epsilon ds(T_i^4 - T_a^4) = 0$$

The above energy balance results are replaced by using the appropriate equation in the following equation.

$$-kA \frac{d\theta}{dx} + hds\theta + \sigma \epsilon ds(T_i^4 - T_a^4) = 0 \dots\dots\dots(2.6)$$

2.2 Calculate surface area and cross-sectional area :-

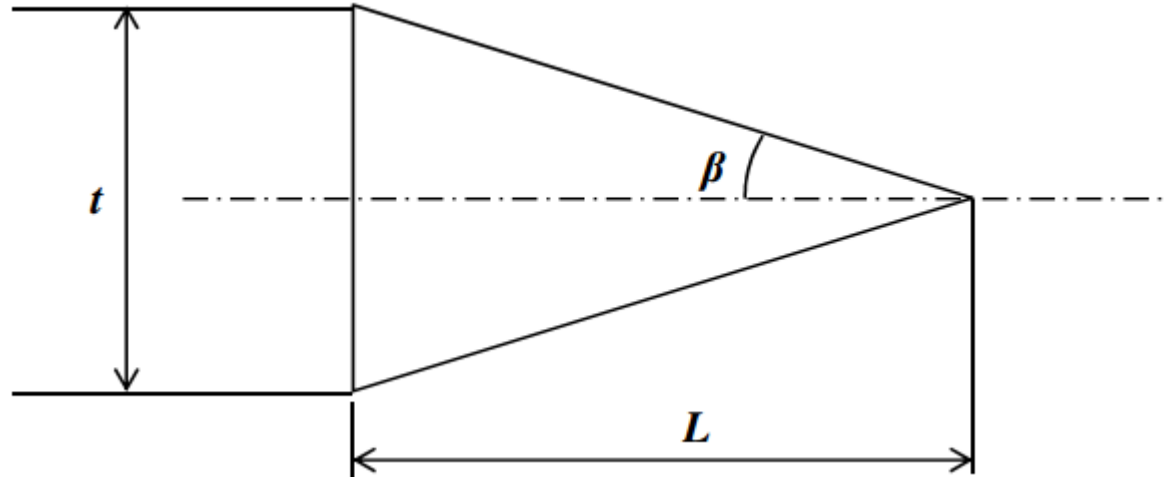


Figure 5: Calculation of surface area and cross sectional area

From Fig 6, we have:

$$\tan\beta = \frac{t/2}{L} \dots\dots\dots 2.7$$

From the above trigonometric relation, semi angle is calculated.

2.2.1 For the interior nodes

a. To Calculate Surface Area

Now,

$$\cos\beta = ds/dx$$

$$\frac{ds}{dx} = \frac{2w}{\cos\beta} \dots\dots\dots 2.8$$

Here also, the equation (2.8) is multiplied by “2” to take account of the dissipation from both lateral surfaces.

b. To Calculate Cross-sectional Area

$$A(x) = \frac{tx}{L} w \dots\dots\dots 2.9$$

$$\frac{dA(x)}{dx} = \frac{tw}{L} \dots\dots\dots 2.10$$

2.2.2 For the tip

a. To Calculate Surface Area

$$\cos\beta = \frac{dx/2}{s}$$

$$S = \frac{2w dx}{2\cos\beta} \dots\dots\dots 2.11$$

b. To Calculate Cross-sectional Area

$$A(1) = \frac{tdx}{2L} w \dots\dots\dots 2.12$$

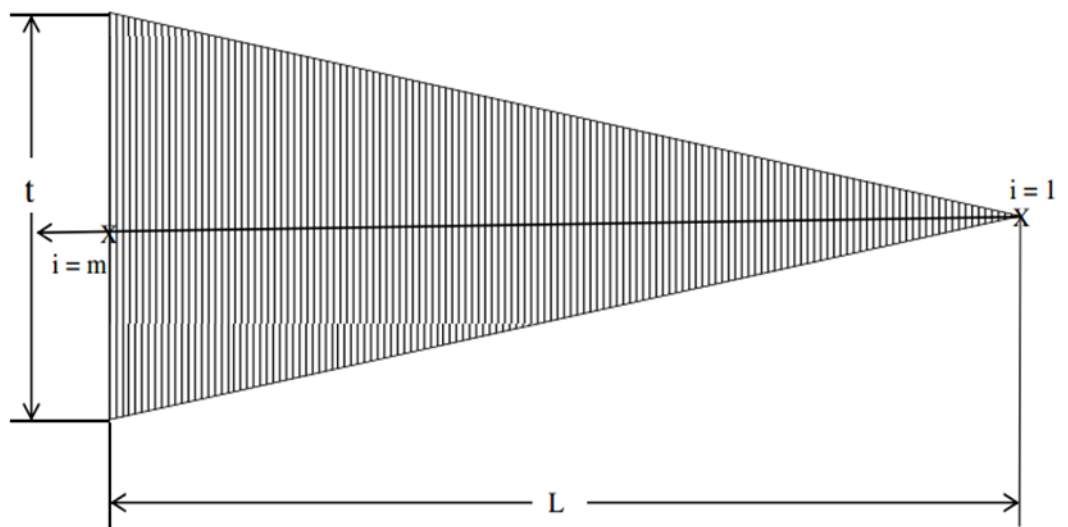
After replacing the appropriate second-order finite-difference analogues with computer code written in C++, Equations (2.2), (2.4) and (2.6).

The surface area relationships of (2.8), (2.9), (2.10), (2.11) and (2.12) are directly incorporated into the forthcoming chapter to obtain the final set of algebraic equations.

3. METHOD OF SOLUTION AND RANGE OF PARAMETERS

The previous chapter evaluated the equations of temperature distribution. These equations are nonlinear ordinary differential equations (ODE). These equations are converted to algebraic forms by substituting appropriate second-order exact finite-difference analogs.

3.1 Discretization of uniform grid control equations



The below obtained algebraic equations are for the uniform grid size.

3.1.1 At the base of the fin

Specify the Dirichlet boundary conditions at the bottom of the fins (temperature known a priori). Equation (2.2) remains unchanged.

$$\theta_m = T_b - T_a \text{ -----} 3.1$$

3.1.2 For the interior nodes

The ordinary differential equation (2.4) derived in Chapter 2 is transformed into an algebraic form by substituting an appropriate second-order exact finite difference simulation, as given below.:

$$\left(\frac{d^2\theta}{dx^2}\right)_i + \frac{1}{A}\left(\frac{dA}{dx}\right)\left(\frac{d\theta}{dx}\right)_i - \frac{h}{kA}\left(\frac{ds}{dx}\right)\theta_i - \frac{\sigma\epsilon}{kA}\left(\frac{ds}{dx}\right)(T_i^4 - T_a^4) = 0$$

By using central difference method—

$$\frac{\theta_{(i+1)} - 2\theta_i + \theta_{(i-1)}}{\Delta x^2} + \frac{L}{t.x.w}\left(\frac{t.w}{l}\right)\left(\frac{\theta_{(i+1)} - \theta_{(i-1)}}{2\Delta x}\right) - \frac{h}{kA}\frac{2w}{\cos\beta}\theta_i - \frac{\sigma\epsilon}{kA}\left(\frac{2w}{\cos\beta}\right)(T_i^4 - T_a^4) = 0$$

$$\frac{\theta_{(i+1)} - 2\theta_i + \theta_{(i-1)}}{\Delta x^2} + \frac{1}{x}\left(\frac{\theta_{(i+1)} - \theta_{(i-1)}}{2\Delta x}\right) - \frac{h}{kA}\frac{2w}{\cos\beta}\theta_i - \frac{\sigma\epsilon}{kA}\left(\frac{2w}{\cos\beta}\right)(T_i^4 - T_a^4) = 0$$

$$\theta_i = \frac{\frac{\theta_{(i+1)} + \theta_{(i-1)}}{\Delta x^2} + \frac{\theta_{(i+1)} + \theta_{(i-1)}}{2x\Delta x} - \frac{\sigma\epsilon}{kA}\left(\frac{2w}{\cos\beta}\right)(T_i^4 - T_a^4)}{\frac{2}{\Delta x^2} + \frac{2hw}{kA\cos\beta}}$$

$$\theta_i = \frac{\frac{\theta_{(i+1)} + \theta_{(i-1)}}{\Delta x^2} + \frac{\theta_{(i+1)} + \theta_{(i-1)}}{2x\Delta x} - \frac{\sigma \epsilon (\frac{2L}{\cos\beta})(T_i^4 - T_a^4)}{ktx}}{\frac{2}{\Delta x^2} + \frac{2hL}{ktx\cos\beta}} \dots\dots\dots 3.2$$

3.1.3 For the Tip

Ordinary differential equation with dissipative tip obtained in Chapter 2 above (2.6). After replacing the appropriate second-order exact finite-difference simulation results, the equation thus obtained leads to

$$\text{Or,} \quad -kA \frac{d\theta}{dx} + hds\theta_i + \sigma \epsilon ds (T_i^4 + T_a^4) = 0$$

By using backward difference method----

$$\theta_i = - \frac{\theta_{(i+2)} + \theta_{(i+1)} - 3\theta_i}{2\Delta x}$$

$$\text{Or,} \quad -kA \left(- \frac{\theta_{(i+2)} + \theta_{(i+1)} - 3\theta_i}{2\Delta x} \right) + hds\theta_i + \sigma \epsilon ds (T_i^4 - T_a^4) = 0$$

$$\text{Or,} \quad \frac{-kA}{2x} (4\theta_{i+1} - \theta_{i+2}) + \sigma \epsilon ds (T_i^4 - T_a^4) = \theta_i \left(- \frac{3kA}{2x} - h \right)$$

$$\theta_i = \frac{\frac{ktw}{4L} \{4\theta_{(i+1)} - \theta_{(i+2)}\} - \frac{\sigma w \epsilon ds (T_i^4 - T_a^4)}{\cos\beta}}{\frac{hwds}{\cos\beta} + \frac{3kw\epsilon}{4L}} \dots\dots\dots 3.3$$

3.2 Discretization of the governing equations for non-uniform grids

To tackle the steep temperature gradients at the base of the fin, a finer mesh size is used, whereas mesh becomes coarser as one move away from the base of the fin. This type of meshing is best achieved by semi-cosine grids.

The equation for the semi-cosine grids is

$$X(i) = \left[1 - \cos \frac{\pi(i-1)}{2(m-1)}\right]L \dots\dots\dots 3.4$$

The Lagrangian polynomial method is employed to discretize the equations obtained for un- equispaced grids. The algebraic forms of the governing equations for the equispaced grids are also can be deduced similarly as above with the help of Lagrangian polynomial method.

3.3 Solution Methodology to algebraic equations

Gauss-Seidel iterative technique is employed to solve the resulting set of discretized equations. Full relaxation (relaxation parameter = 1) is employed on temperature during iterations. During the iteration process, the residuals are monitored and the solution is considered to be converged when the residue pertaining to the local temperature at any point in the computational domain becomes less than a prescribed minimum that is taken to be 10^{-8} .

Here, the residue is defined as:

$$\left| \frac{T_{new} - T_{old}}{T_{old}} \right| \times 100 < 10^{-8}$$

The numerical solutions presented in this report are obtained by choosing equispaced grid system for calculations. C⁺⁺ computer code is written for solving the present project problem.

3.4 Range of parameter

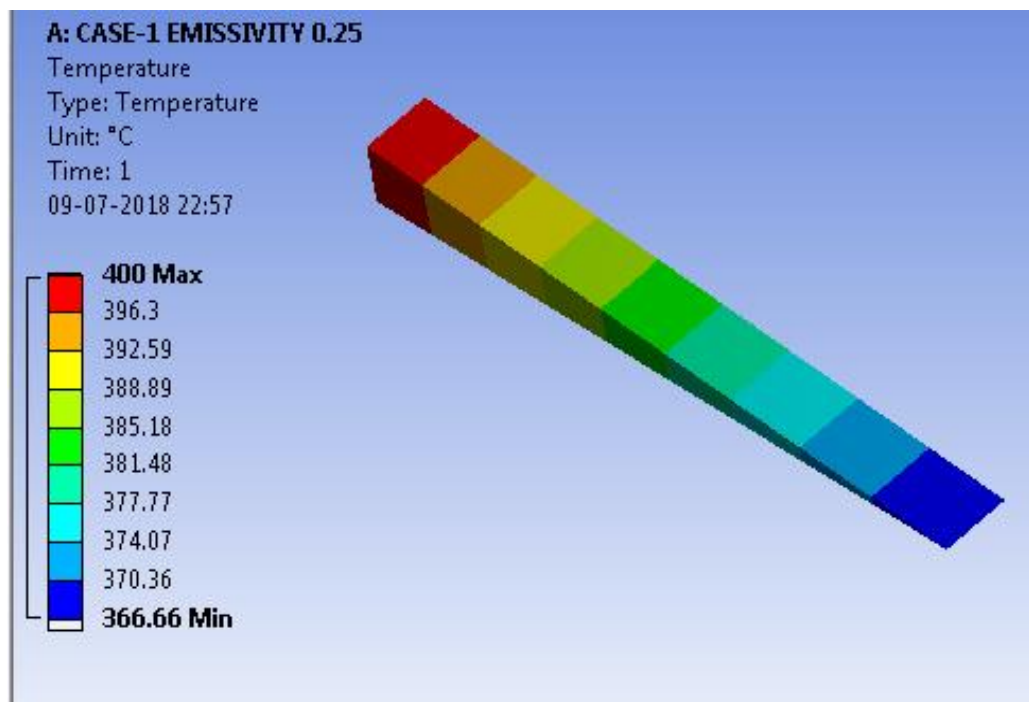
The length (L) of the triangular fin is fixed to be 10 cm and width is fixed to be 1 cm. Thickness at the base of the fin is 1 cm, i.e. Aspect Ratio (AR) is varied from 10. The temperature of the air is being taken to be 22^oC.

The emissivity is varied from 0.05-0.85. The lower value of emissivity signifies the poor emitter and the upper value signifies the good emitter. Convection heat transfer coefficient is varied from 5 W/m C to 15 W/m C, where 5 W/m C refers to the asymptotic free convection limit. Thermal conductivity is chosen from 0.72 W/m C to 205 W/m C, where 0.72 W/m C refers to very poor conductor of heat and 205 W/m C refers to very good conductor of heat that is aluminium. There is no heat generation within the fin and heat which is conducted at the base is being convected and radiated to the ambient.

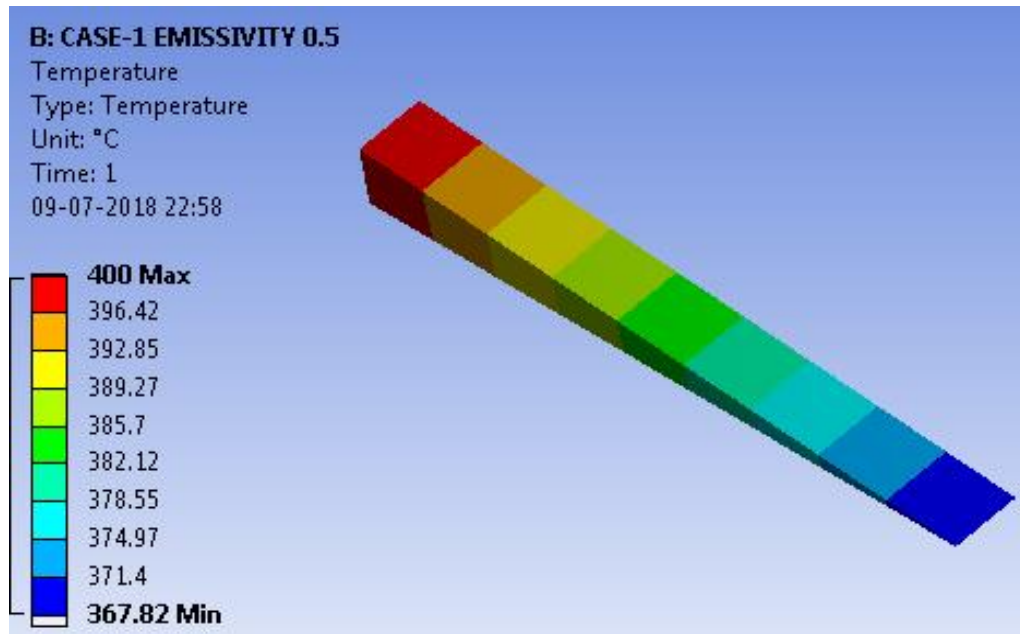
4. OBSERVATION THROUGH ANSYS

The ANSYS is a computer based analysis software which is known for its capability Finite Element Analysis.

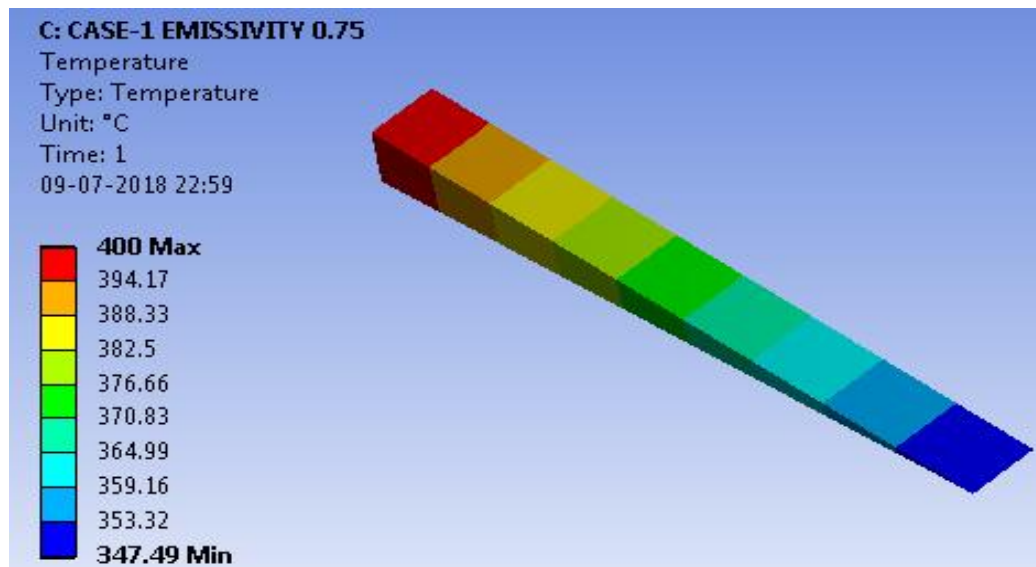
4.1 Variation of temperature along length of triangular fin for varying Emissivity. For $k= 205 \text{ w/m C}$, $h= 5 \text{ w/m}^2 \text{ C}$, Temperature= 400°C



Graph 1: Emissivity = 0.25



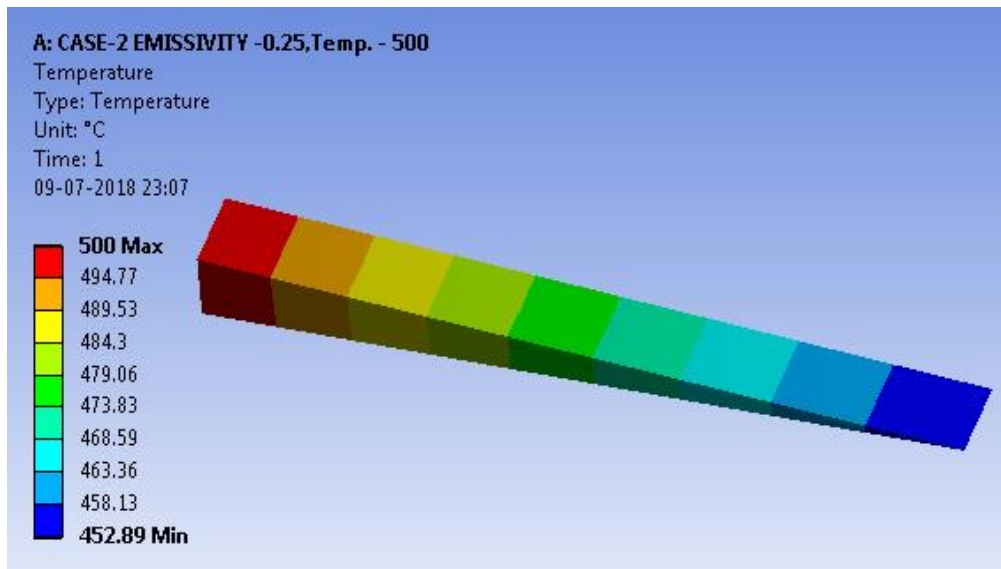
Graph 2: Emissivity = 0.5



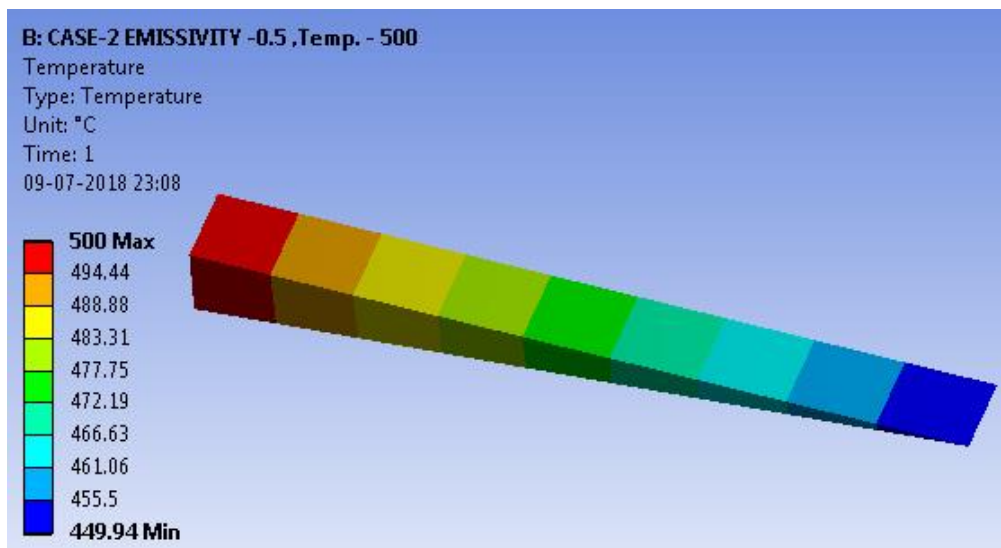
Graph 3: Emissivity=0.75

The Graph 1,2& 3 shows the variation of temperature along the length for varying emissivity and we can say that the temperature variation is more for higher emissivity value.

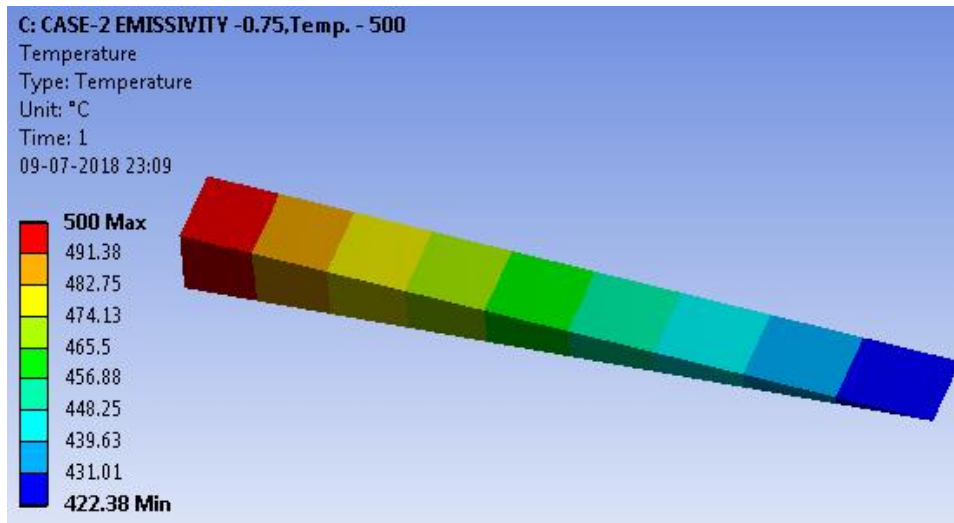
4.2) Variation of temperature along length of triangular fin geometry for varying Emissivity for thermal conductivity $K=205\text{w/m C}$, $h=5\text{w/m}^2\text{c}$ & Temperature= 500°C



Graph 4: Emissivity= 0.25



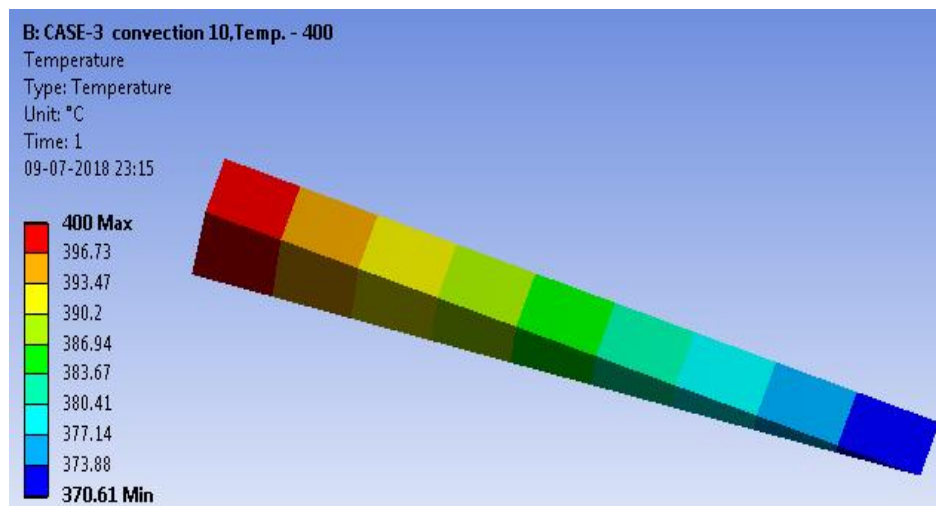
Graph 5: Emissivity= 0.5



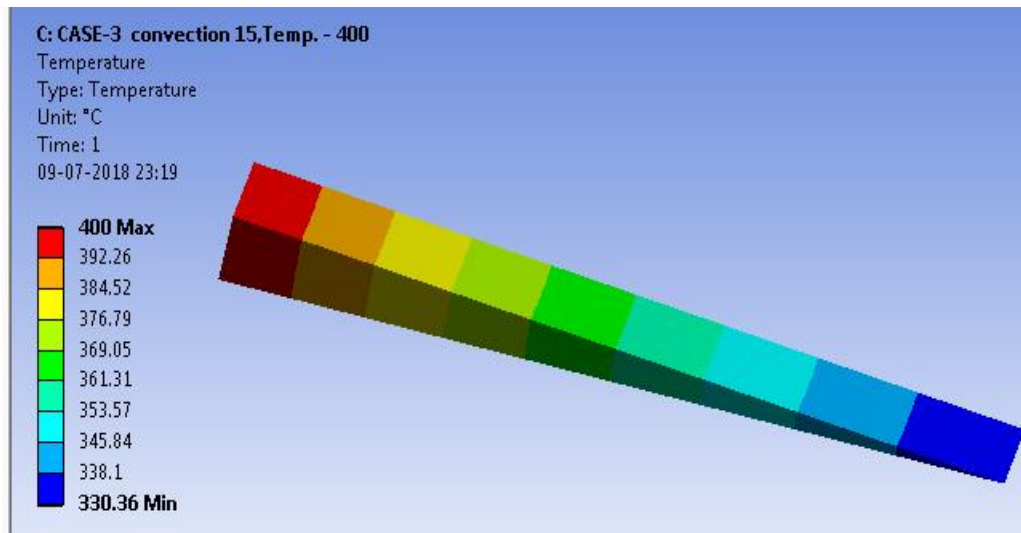
Graph 6: Emissivity= 0.75

Graph 4, 5 & 6 shows that the variation of temperature along the length of triangular fin geometry at same k , h & ϵ as in case 1, but temperature is 500°C , for varying emissivity.

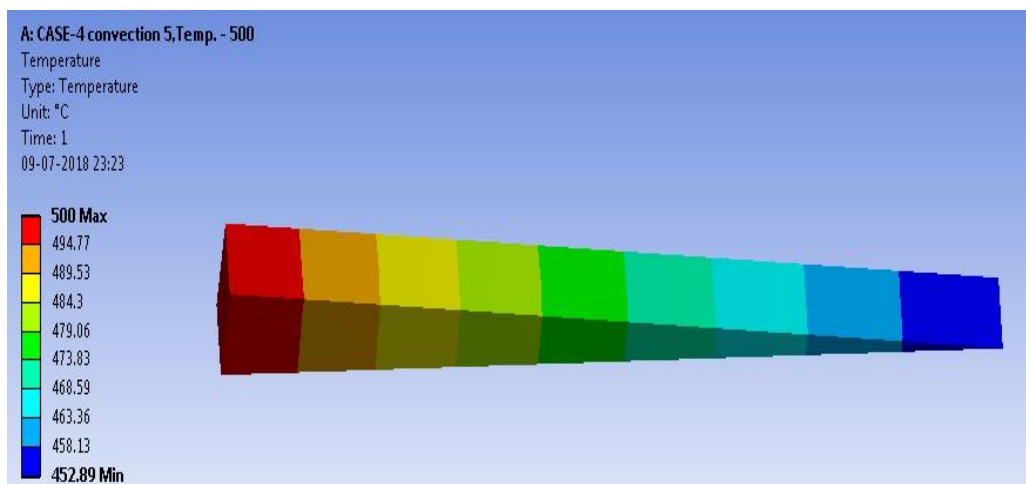
4.3) Variation of temperature along the length of triangular fin geometry for varying convective coefficient h provided that the emissivity=.25, and conduction heat transfer coefficient $k=205\text{w/m}^{\circ}\text{C}$.



Graph 7) Convective Coefficient $h=10\text{w/m}^2\text{C}$



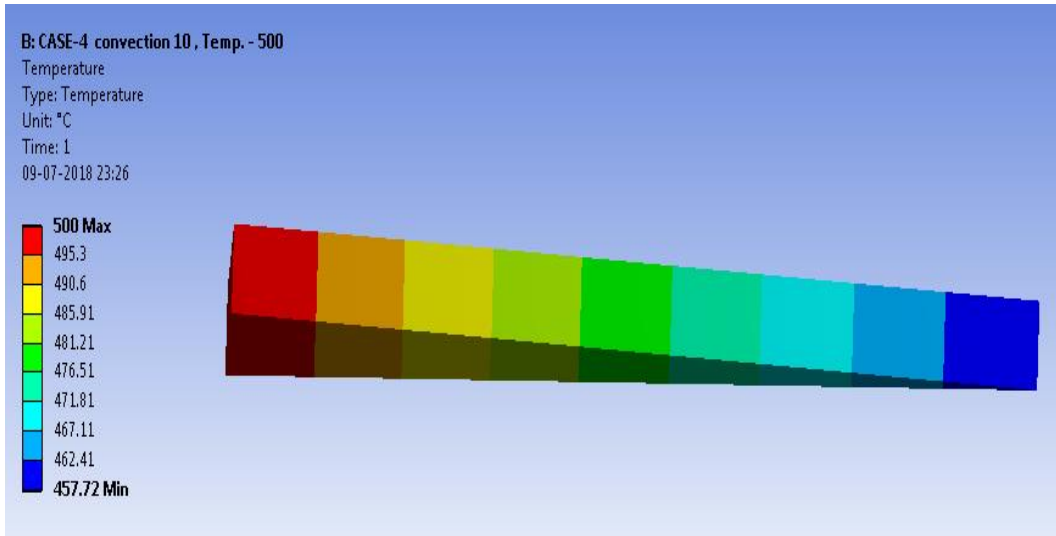
Graph 8) Convective Coefficient $h= 15\text{w/m}^2\text{°C}$



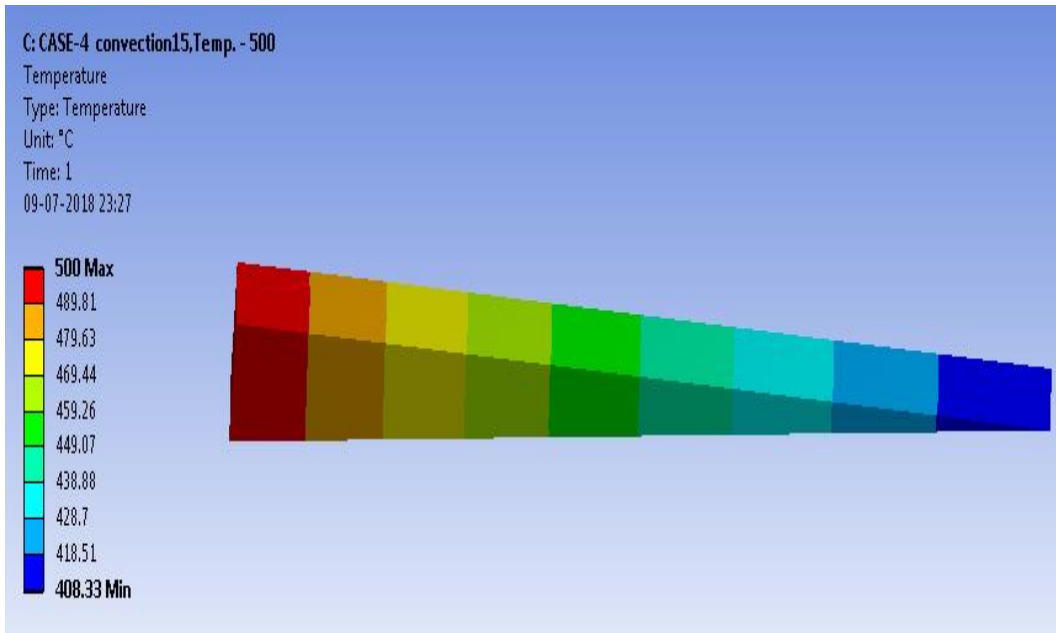
Graph 9) Convective Coefficient $h= 5\text{w/m}^2\text{°C}$

Graph 7, 8 & 9 shown the variation of temperature / distribution of temperature along the length of fin for varying value of h at same value of k , t_b & ϵ in three cases above. As h increase lowest temperature achieved at end of fin.

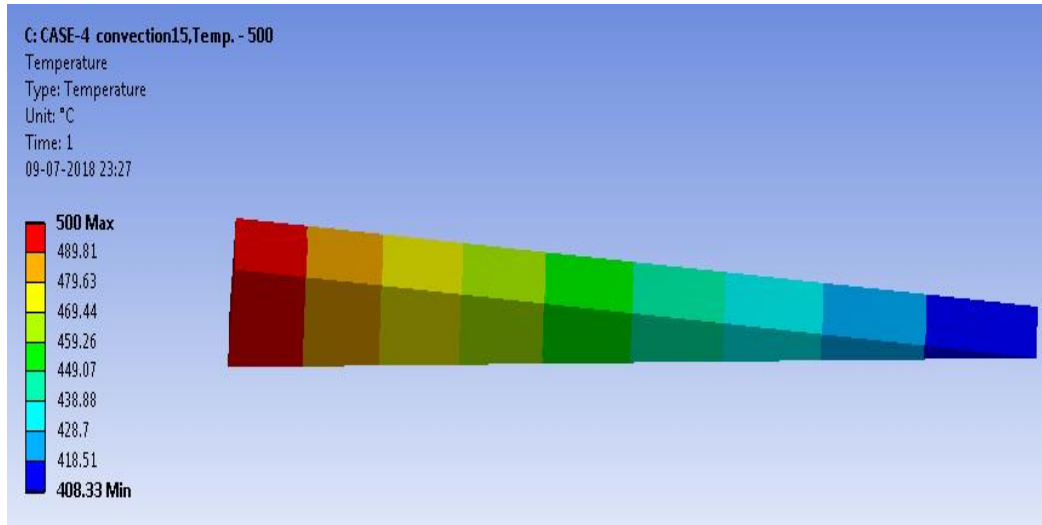
4.4) Distribution of Temperature along the length of fin for varying convective coefficient when $k=205\text{w/m}^2\text{°C}$, $\epsilon=0.25$ & $T_b= 500\text{°C}$.



Graph 10) Convective Coefficient $h=10 \text{ w/m}^2\text{°C}$



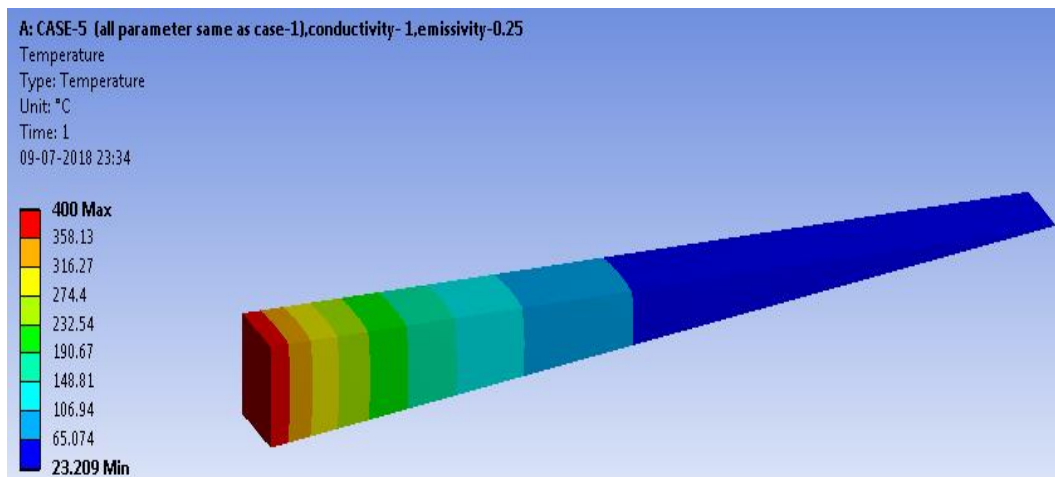
Graph 11) Convective Coefficient $h= 15\text{w/m}^2\text{°C}$



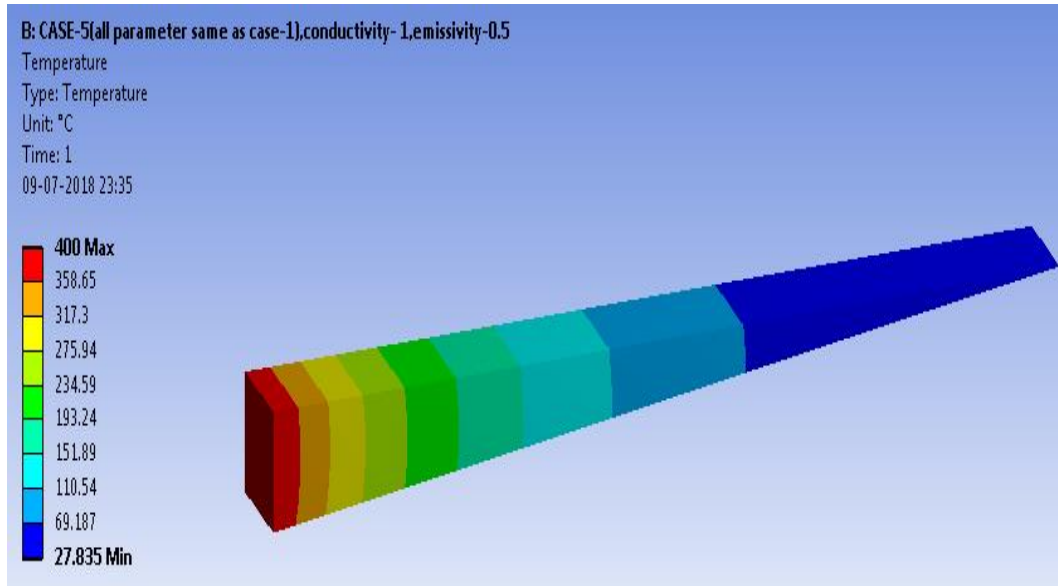
Graph 12) Convective Coefficient $h= 5w/m^2^{\circ}C$

From the graph of 10, 11 &12, distribution of temperature along the length of fin ,all condition are same and value of parameters are same, but here temperature is $500^{\circ}C$ & variation is less along the fin as compare to above case.

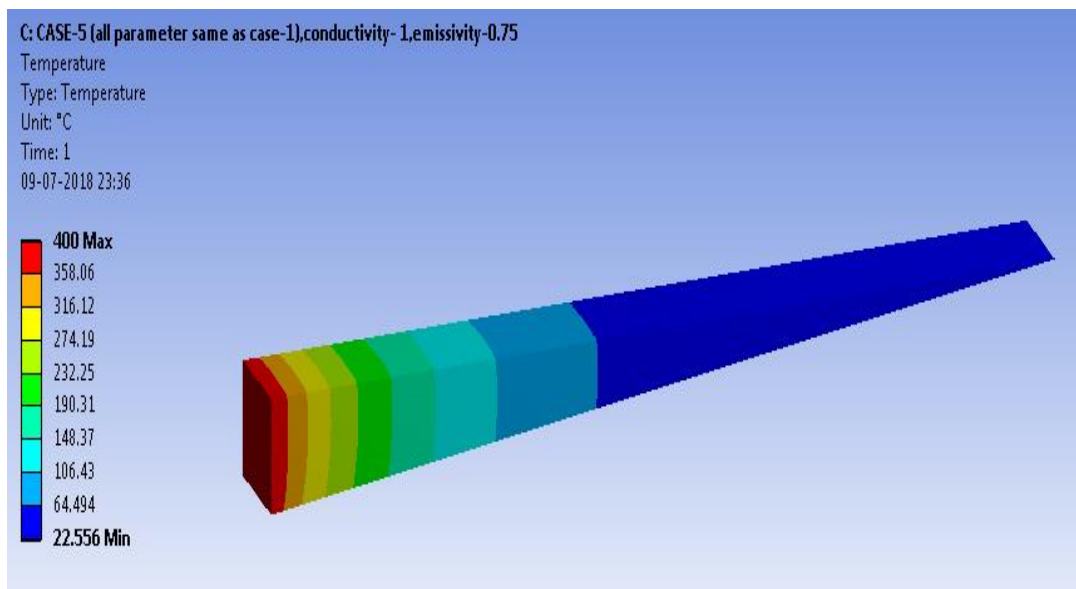
4.5) Temperature Distribution along the length of fin for varying emissivity when $k= 1w/m^{\circ}c$, $h= 5w/m^2^{\circ}c$, $T_b= 400^{\circ}C$.



Graph 13) Emissivity = 0.25



Graph 14) Emissivity= 0.5



Graph 15) Emissivity= 0.75

This case which contains graphs 13, 14 & 15, having the same value of parameters like h , T_b & ϵ , only one difference is case 1 having $k=205\text{w/m}^\circ\text{c}$, & for this case $k=1\text{w/m}^\circ\text{c}$, but the distribution of temperature is more in this, achieved lowest temperature at the end of fin also in this case compare to case 1.

5. RESULTS AND DISCUSSION

Before conducting the parametric study on the current triangular fin problem, based on the exhaustive grid convergence study, the optimal grid convergence required for the discretization of the computation domain is obtained.

5.1 Grid sensitivity test

In the present project work problem, the grid convergence analysis is carried out in two phases, which includes both equispaced and un-equispaced grids. The equispaced grid study as shown in fig. is performed for a fixed set of parameters, viz., $k = 205 \text{ W/m C}$, $h = 5 \text{ W/m}^2 \text{ C}$, $C = 0.25$, $L = 10 \text{ cm}$, $t = 1 \text{ cm}$, $AR = 10$ and $w = 1 \text{ cm}$. In the first stage of the above study as given by table 6-1, equispaced grids the number of grids along the x-direction i.e. m is varied. The table 6-1 highlights that the % change in temperature at the mid-node decreases from 0.1272% to 0.1269% as the grid size is increased from 91 to 141, while a further increase of m to 151 shows still increase in temperature also followed by an increase in the percentage change in the absolute value. From this equispaced grid study it can be noticed that, there is a breakeven point at $m=141$. Therefore $m =141$ are opted for the further studies

Table 5- 1 Triangular fin - equispaced grids ($k = 205 \text{ W/m C}$, $h = 5 \text{ W/m}^2 \text{ C}$, $\epsilon = 0.25$, $L = 10 \text{ cm}$, $t = 1 \text{ cm}$, $AR = 10$ and $w = 1 \text{ cm}$)

| S.N | Grid Size M | Mid-node Temperature in $^{\circ}\text{C}$ | % abs change |
|-----|-------------|--|--------------|
| 1 | 91 | 93.5501 | 0.127259417 |
| 2 | 101 | 93.6692 | 0.127311462 |
| 3 | 111 | 93.7883 | 0.127149586 |
| 4 | 121 | 93.9075 | 0.127094744 |
| 5 | 131 | 94.0268 | 0.127039906 |
| 6 | 141 | 94.1462 | 0.126985072 |
| 7 | 151 | 94.2658 | 0.12703646 |

The table 5-2 shows the grid test results obtained with un-equispaced, semi-cosine grids for a fixed set of parameters, viz., $k = 205 \text{ W/m C}$, $h = 5 \text{ W/m}^2 \text{ C}$, $\epsilon = 0.25$, $L = 10 \text{ cm}$, $t = 1 \text{ cm}$, $AR = 10$ and $w = 1 \text{ cm}$. Here grid size is varied from 121 to 211 and the variation in the mid node temperature and percentage change (abs.) value is calculated. The results of the table shows that there is continuous increase in the mid node temperature and percentage change in the absolute value decreases continuously. Also the percentage change is large compare to the equispaced grid system.

Table 5- 2 Triangular fin - un-equispaced grids ($k = 205 \text{ W/m C}$, $h = 5 \text{ W/m}^2 \text{ C}$, $\epsilon = 0.25$, $L = 10 \text{ cm}$, $t = 1 \text{ cm}$, $AR = 10$ and $w = 1 \text{ cm}$)

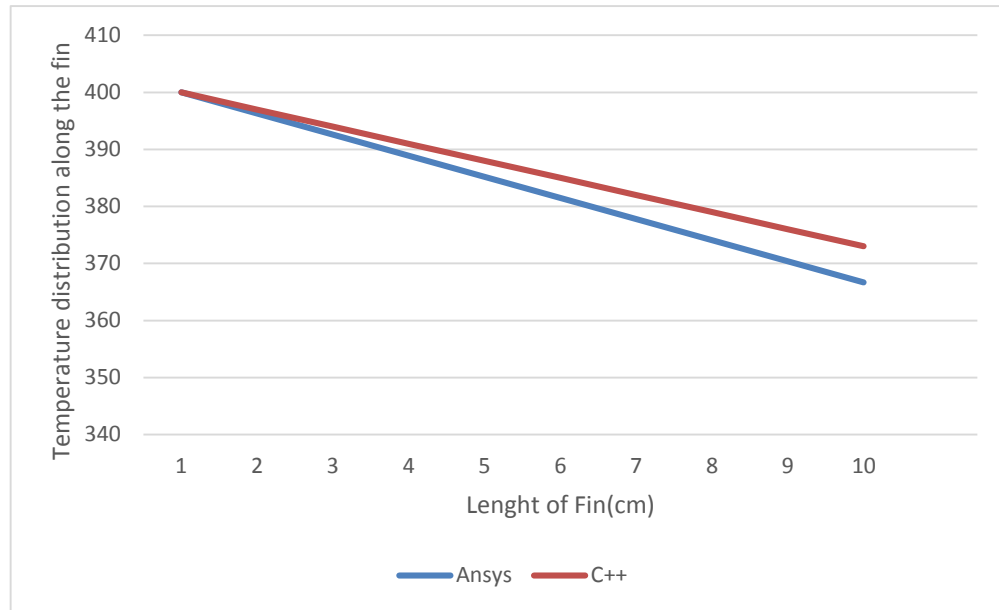
| SN | Grid Size M | Mid-node Temperature in ° C | % change (abs) |
|----|-------------|--------------------------------|----------------|
| 1 | 121 | 94.6828 | 0.191000642 |
| 2 | 131 | 94.8621 | 0.189369136 |
| 3 | 141 | 95.0401 | 0.187640796 |
| 4 | 151 | 95.2167 | 0.185816303 |
| 5 | 161 | 95.3917 | 0.183791289 |
| 6 | 171 | 95.5651 | 0.181776821 |
| 7 | 181 | 95.7366 | 0.179458819 |
| 8 | 191 | 95.9063 | 0.177257183 |
| 9 | 201 | 96.0739 | 0.1747539 |
| 10 | 211 | 96.2394 | 0.172263227 |

By varying the values of h , k , grid convergence test is performed for un-equispaced grids. The results obtained by this study are varying much more compared with the tabulated values. As equispaced grid system gives better convergence and breakeven point, it is incorporated for the further analysis. The optimum value of grid number is freeze to $m=141$. Now we can observe the different variations such as emissivity, thermal conductivity, convection heat transfer coefficient, base temperature along the length of fin by C^{++} observation as well as ansys results interpretations.

Comparison Between Ansys result & C++ result

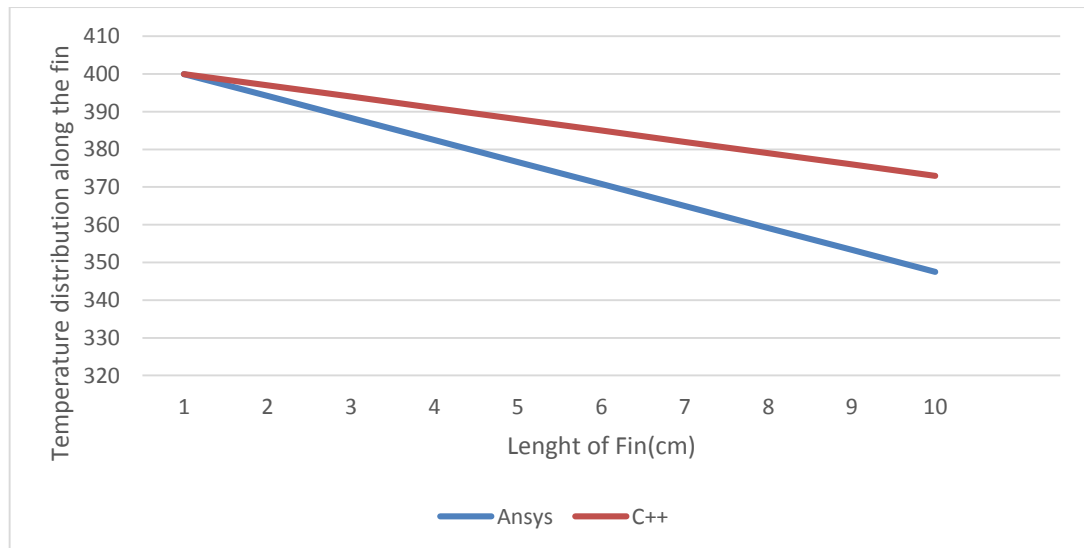
5.2.1- When Base Temperature is 400°C , $k=205\text{w/mC}$ and $h= 5\text{w/m}^2\text{C}$.

(a) When Emmissivity(ϵ)= 0.25



Graph 16)

(b) When Emmissivity(ϵ)= 0.75

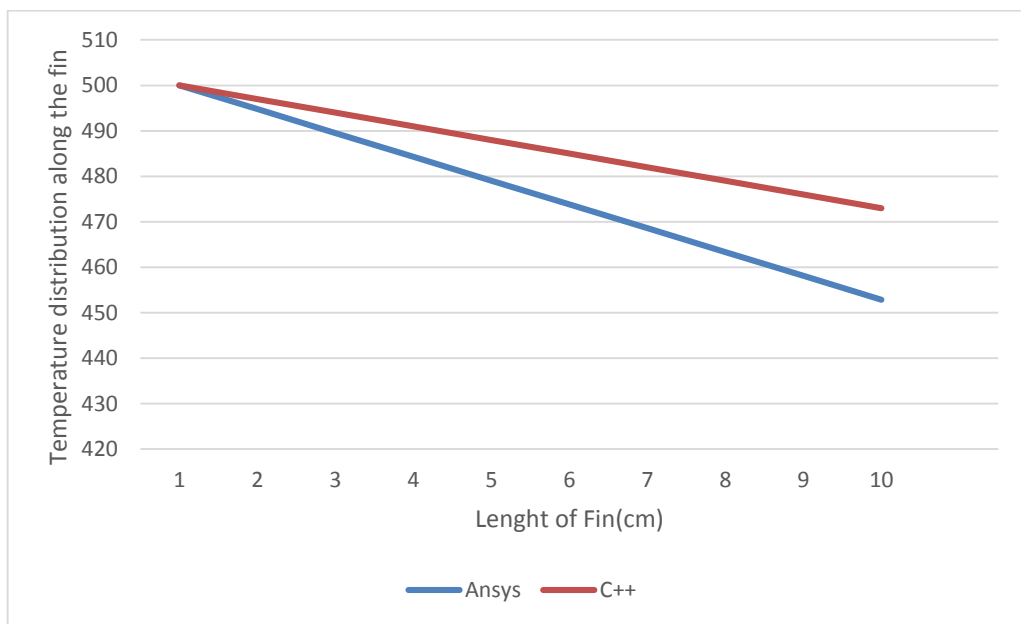


Graph 17)

From figures 16 and 17, results obtained is that as we increased emissivity heat transfer also increased, and temperature difference between c++ & ansys also increased as emissivity increased.

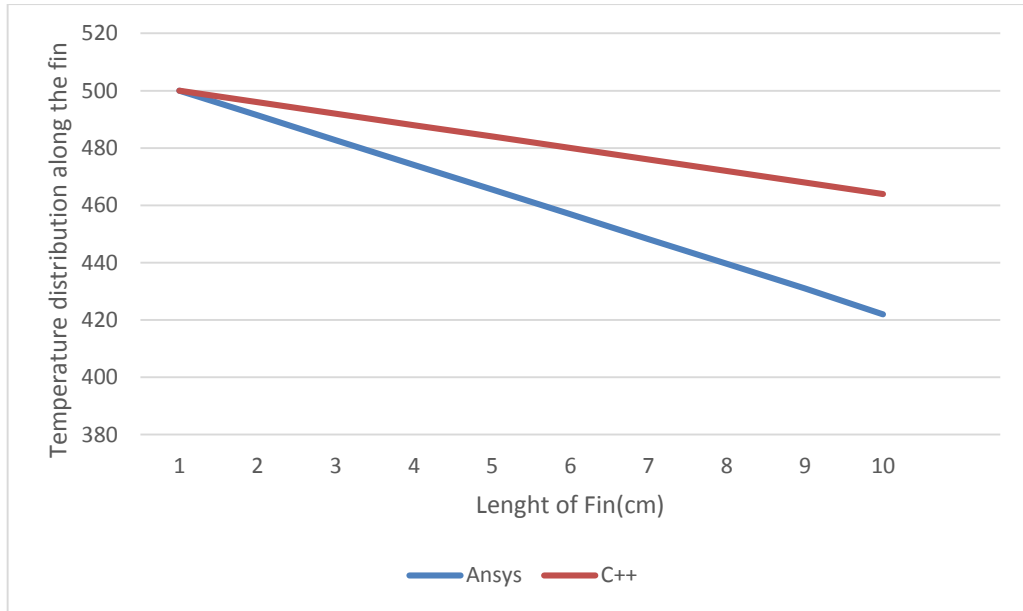
5.2.2)- When Base Temperature $T_b = 500^\circ\text{C}$, $K = 205\text{W/m}^\circ\text{c}$ & $h = 5\text{W/m}^2\text{c}$.

(a):- Emissivity= 0.25



Graph 18)

(b) When Emissivity =0.75

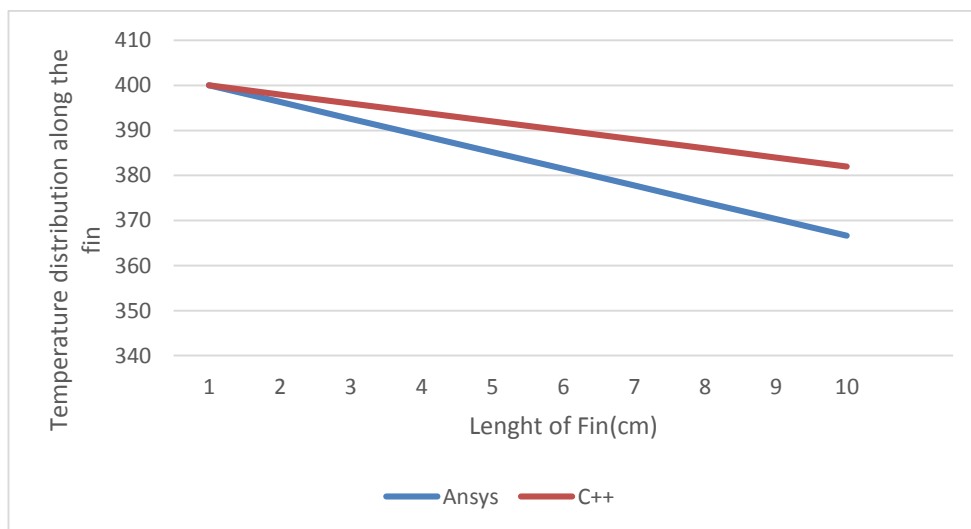


Graph 19)

In figure 18 & 19, the temperature distribution over length of triangular fin is more as compared to when base temperature is 400°C, and more temperature line gap between c++ & ansys in this case.

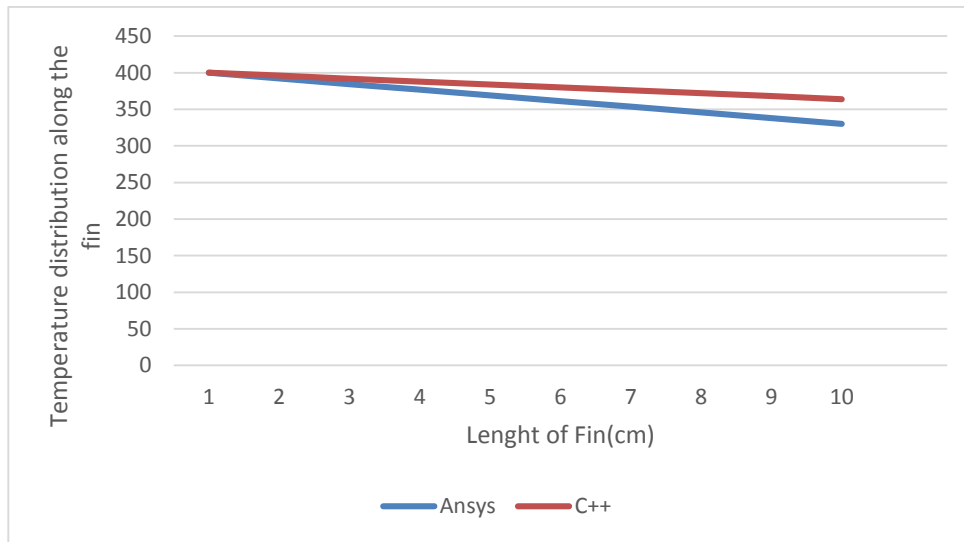
5.2.3) When Base Temperature $T_b = 400$, $K = 205 \text{ W/m}^\circ\text{C}$, $h = \text{W/m}^2\text{C}^\circ$ & Emissivity (ϵ) = 0.25.

(a) When $h = 5 \text{ W/m}^2\text{C}^\circ$



Graph 20)

(b)- When $h = 50 \text{ W/m}^2\text{C}^\circ$

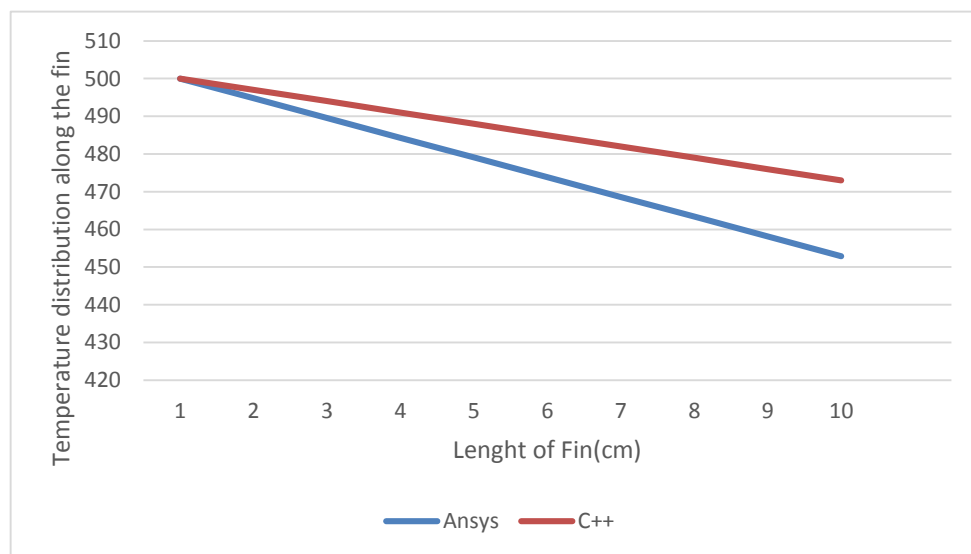


Graph 21)

As the value of h increased temperature distribution line gap between c++ & ansys decreased because of large rate of convective heat transfer. As shown in figure 20 & 21 respectively.

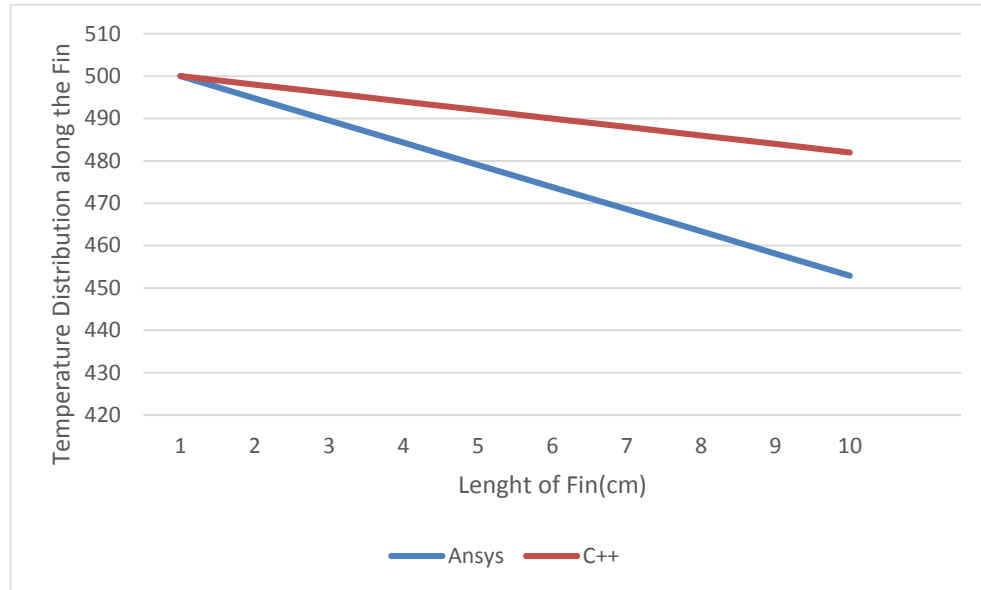
5.2.4) When Base Temperature $T_b = 500^\circ\text{C}$, $K = 205\text{W/m}^\circ\text{C}$, Emissivity(ϵ) = 0.75.

(a) When $h = 5\text{W/m}^2\text{C}$



Graph 22)

(b) When $h= 50\text{W/m}^2\text{C}$.



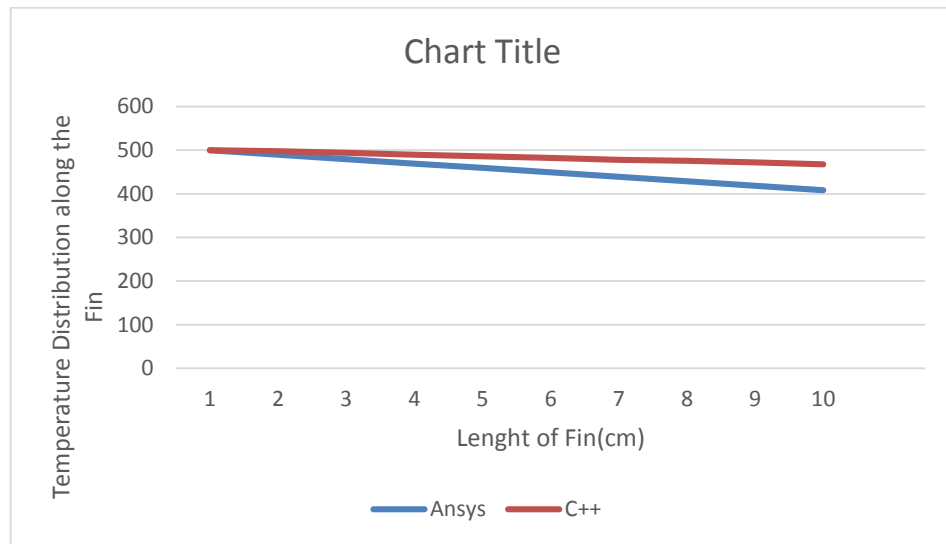
Graph 23)

In this case result is reversed as compared to the results obtained in previous case, as shown in figure 20 & 21 respectively. Graph 20, 21, 22 & 23 shows the nature of variation of local temperature along the triangular fin in the various regions of convection, where $h=5 \text{ W/m}^2 \text{ C}$ refers to asymptotic free convection limit and $h=50 \text{ W/m}^2 \text{ C}$ refers to asymptotic forced convection limit. The study is performed for a fixed set of input parameters viz., $k = 205 \text{ W/m C}$ and $AR = 10$. Two different values of heat transfer coefficient (h) are chosen viz., $5 \text{ W/m}^2 \text{ C}$ & $50 \text{ W/m}^2 \text{ C}$. It can be observed from Graph22 & 23 that the temperature decreases continuously for increasing value of h , which is obvious as the h value increases, the fin dissipates more amount of heat to the ambient by convection heat transfer. Also it can be noticed that for a given value of h , an increase in emissivity from 0.25 to 0.75 shows a large drop in temperature highlighting the effect of heat transfer by radiation. However, the effect of radiation is dominant in the region of lower heat

transfer coefficient ($h=5 \text{ W/m}^2 \text{ C}$), which is the asymptotic free convection limit. Further, increase in film coefficient ($h=50 \text{ W/m}^2 \text{ C}$, refers to forced convection regime) dominates the radiation which is shown in the upcoming

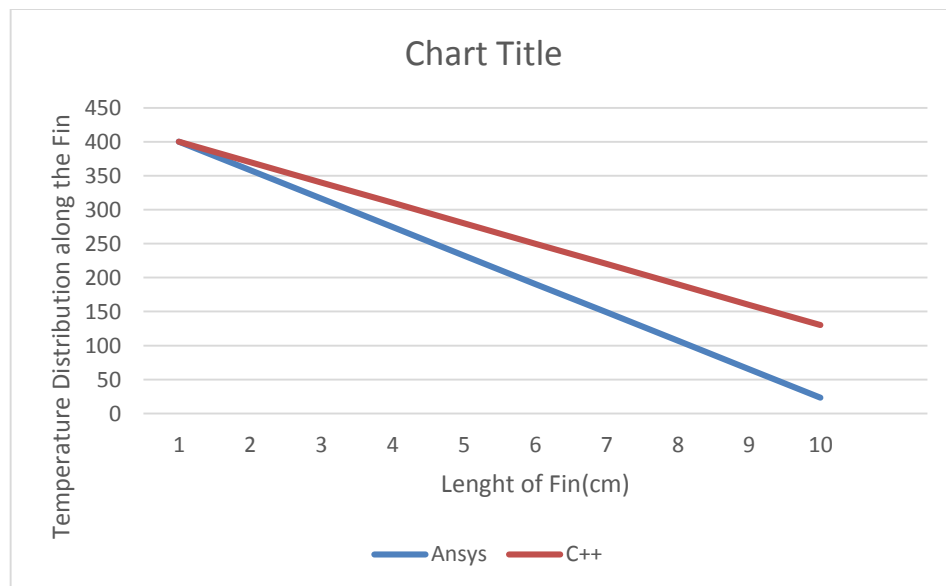
5.2.5) Base Temperature $T_b= 400^\circ\text{C}$, $K= 1\text{W/m}^\circ\text{C}$, $h= 5\text{W/m}^2^\circ\text{C}$.

(a) When Emissivity (ϵ) = 0.25



Graph 24)

(b) When Emissivity (ϵ)= 0.75



Graph 25)

Results obtained from this case compared with case (5.2) because between these to case only one parameter vary which is K, value of k for case (5.2) is $205 \text{ W/m}^\circ\text{C}$, and value of k for this case is the lowest value of k(poor conductivity coefficient) is $1 \text{ W/m}^\circ\text{C}$, temperature distribution line of c++ and ansys is more downward and achieved less less temperature , and more heat transfer in this case, compared to case (5.2). Two different values of surface emissivity are chosen viz., 0.25 and 0.75 for Two different values of thermal conductivity (k) viz., 205 W/m C , and 1 W/m C . It can be noticed that, the local temperature along the fin decreases continuously from a maximum value at the base to a minimum value at the tip. However, for the lower values of thermal conductivity ($k = 1 \text{ W/m C}$), the temperature profile shows an exponential behaviour and also steep gradients, which is as shown in Graph 24 through observation of C++ & the result of ANSYS for same conditions is also shown in Graph 25. The Graph 24 further shows that, the local temperature profiles for different values of emissivity are merging at about 0.08 m from the tip of the fin. Also, the local temperature peters down to the ambient value at a distance of about 0.1 m , which shows that, this length itself behaves as the infinite length for the fin. Graph 24 and Graph 25 shows the type of variation of local fin temperature along the fin for various values of ϵ and $k=205 \text{ W/m C}$ (i.e. using C++ and ANSYS software respectively)and for a fixed set of input values $h=5 \text{ W/m}^2 \text{ C}$ and $AR=10$. In general, fins are made from aluminium having thermal conductivity at around 205 W/m-C . From the Graph 1& Graph 2 it can be witnessed that, the fin approaches isothermal nature compared to Graph 24& Graph 25 using C++ and Graph 3 & 4 using ANSYS respectively and because of the higher value of thermal conductivity. Also it can be observed that, as the increases, the temperature drops down, which is attributed to the fact that, as increases the radiation heat transfer is intensified.

6. CONCLUDING REMARKS AND SCOPE FOR FUTURE WORK

This project aims to use finite-difference method (FDM) to perform various simulations on combined conduction-convection and radiation from triangular fin geometry. It is well known that while non-uniform fins such as (i) triangular fins and (ii) annular fins are considered in various physicist literatures, few studies have attempted to incorporate radiation interactions into their investigations.

In this regard, the current project work successfully studied the interaction between radiation and conjugate convection (combination of conduction and convection) and the geometry of triangular fins.

Computer code in C++ has been written to solve this problem. The effects of various independent parameters, such as thermal conductivity (k), fin surface emissivity (ϵ), convective heat transfer coefficient (h) and aspect ratio (AR), were thoroughly studied. Some of the results include

- Local temperature distribution along the fin using C++
- Local temperature distribution along the fin using ANSYS

From the above studies, it can be concluded that:

During free convection (ie, low h , 5 to 15W/m² C), radiation cannot be neglected because radiation heat transfer also plays a major role in free convection.

The thermal conductivity of the fin material should be chosen such that it has minimal resistance to heat transfer rates and allows the fins to be isothermal.

Better surface finish results in higher surface emissivity in order to increase the rate of heat transfer from the fins through the radiation pattern.

The aspect ratio (AR) should be larger in order to obtain greater efficiency and effectiveness from the heat sink. For this reason, thin, wide and closely spaced fins are used this conclusion from studied various references and book, and analysis of this done in this report.

In addition, the material of the fins should be chosen to be lightweight, economical, and provide manufacturing flexibility.

7.1 Scope for Future Work

Taking into account fluids around the computational domain, current project work may become more complex. This makes the problem even more complicated because one may have to consider the relevant fluid flow and energy equations and the related boundary conditions as a temperature along the temperature of the fins. In addition, the transient response of fins that occur in most engineering problems can be studied. By applying analytical methods and comparing them with C++ results and ANSYS results, the project can be further studied.

In addition, the temperature of each point on the actual model can be measured by a thermocouple, and the percentage error and ANSYS result of C++ programming can be determined.

REFERENCES

1. S. Mirapalli, P.S. Kishore, "Heat Transfer Analysis on a Triangular Fin", IJETT-Volume 19, Jan 2015.
2. M. Sudheer, G.V. Shanbhag, P. Kumar, S. Somayaji, "Finite element analysis of thermal characteristics of annular fins with different profiles:", ARPN Journal of Engineering & Applied science, Vol 7 No. 6, ISSN 1819-6608, June 2012.
3. G.C. Rao, N.V. Rao, K.C. Das, " simulation studies on multi-mode heat transfer from an open cavity with a flush mounted discrete heat source. International Journal Mass Transfer 44:727-737.
4. G.C. Rao, C. Balaji, S.P. Venkateshan , " conjugate mixed convection with surface radiation from a vertical plate with a discrete heat source", ASME J Heat Transfer 123:698-702. Jan 2011.
5. A.E. Zinnes, " The coupling of conduction with laminar natural convection from a vertical flat plate with arbitrary surface heating," ASME J Heat Transfer,1970, 92:528-534,
6. V. Dharma Rao, S.V. Naidu, B. Govinda Rao and K.V. Sharma, October 24-26," Heat transfer from a horizontal fin array by natural convection and radiation a conjugate analysis", Proceedings of the World Congress on Engineering and Computer Science 2007 WCECS 2007, San Francisco, USA, Oct 2007
7. A.A. Dehghan, M. Behnia, " combined natural convection conduction and radiation heat transfer in a discretely heated open cavity", ASME J Heat Transfer,1996, 123:698-702, Feb 1996.
8. S. Abrate, P. Newnham," Finite element analysis of triangular fins attached to a thick wall" Mechanical and Aerospace Engineering, Engineering Mechanics Department, University of Missouri-Rolla, Rolla, MO 65401, U.S.A, June 1994.
9. S.S. Rao, "Overview of Finite Element Method", Department of Mechanical and Aerospace Engineering, University of Miami, Coral Gables, FL, United States, 2004
10. J. Ma, Y. Sun, B. Li, "Simulation of combined conductive, convective and radiative heat transfer in moving irregular porous fins by spectral element method", International journal of thermal science, 2017
11. M.K. Thompson, J.M. Thompson, "Interacting with ANSYS", Ansys mechanical for APDL finite element analysis, 2017.
12. Interacting with ansys, "Mechanical APDL Operations Guide: Chapters 2&4 Mechanical APDL Command Reference: Chapters 1&3",
13. M. P. Shah, K. S. Mehra, S. Gautam, P. Negi, "Transient and Steady State Analysis of Fin Using FEM for Different Material", IRASET Vol.2Issue VI, ISSN: 2321-9653, June 2014.
14. R.S.K. Reddy, K.G. Rajulu, S.M.J. Basha, E.V. Gowd, P.V. Prathap, C.N.V. Vandhan, "Thermal Analysis of Pin Fin with Different Shape Forms using ANSYS", IJESC, Volume 7 Issue No.5, 2017.

15. S. H. Barhatte, "Experimental and Computational Analysis and Optimization for Heat Transfer through Fins with Different Types of Notch", *Journal of Engineering Researches and Studies*, Vol. II, 133-138, 2011.
16. R. Gupta, R. Kumar, P.K. Verma, "Heat Transfer Analysis of Engine Cylinder Fins Having Triangular Shape", *International Journal of Scientific & Engineering Research*, Volume 7, Issue 5, ISSN 2229-5518, May 2016.
17. M. Jain, M. Sankhala, K. Patidar, L. Aurangabadkar, "Heat Transfer Analysis And Optimization Of Fins By Variation in Geometry," *IJMPE*, Volume-5, Issue-7, ISSN: 2320-2092, July 2017.
18. Cengel, Yunus, Boles, A. Michael," McGraw Hill Educatin," 2008.
19. P.K. Nag," Heat and Mass Transfer," Tata McGraw Hill, 2008.
20. Domkundwar & Domkundwar,". Heat and Mass Transfer", Data Book: Dhanpat Rai and Co., (pp. 3.2, 3.5, 3.13), 2008.
21. A. Aziz, "Optimum dimensions of extended surfaces operating in a convective environment", *Appl. Mech. Rev.* 45, 155-173, 1992.
22. A. Aziz and H. Nguyen. "Two-dimensional effects in a triangular convecting fin", *AIAA J. Thermophys.* 6, 165-167, 1992.
23. W. Lau and C. Tan, "Errors in one-dimensional heat transfer analysis in straight and annular fins", *J. Hear Transfer* 549-55 1,1993.
24. D. C. Look and H. S. Kang, "Optimization of a thermally non-symmetric fin", Preliminary evaluation. *Int. J. Heat Mass Transfer* 35, 2057-2060, 1992.
25. D. C. Look, "Separation of variables on a triangular geometry", *Q. J. appl. Math.* 1, 141-148, 1992.

ANNEXURE A.

The programming in C++ is as follows:

```
#include<iostream>
#include<iostream>
#include<stdio.h>
#include<math.h>
#include<fstream>
#include<conio.h>
using namespace std;

int main()
{
int i,n=21;
long double x[500],tt[500],tb,ta,h,k,l=10,sigma=5.67*0.00000001,emis,
t=1,w=1,cosb,
b=1,dx,tn[300],to[300],delta[300],eps=.00000001,big,error[300],d[300],iter,n
iter=0;
ofstream fout ("Fin.xls");
cout<<"enter the value of tb=";
cin>>tb;

cout<<"enter the value of ta=";
cin>>ta;

cout<<"enter the value of h=";
cin>>h;

cout<<"enter the value of k=";
cin>>k;
cout<<"enter the value of emissivity=";
cin>>emis;

dx=(1/(n-1));
x[1]=dx;
cosb=2*(sqrt(t*t/l*1))/t;

for(i=1;i<=n;i++)
```



```

x[i+1]=(x[i]+dx);

for(i=1;i<=n;i++)

to[i]=30;

do
{
iter=niter+1;
for(i=1;i<=n;i++)
{

if(i==1)
{

tn[i]=((((k*t*w)/(4*1))*((4*to[i+1])-to[i+2]))-
((sigma*emis*w*dx)/(cosb)*(((to[i]+ta)*(to[i]+ta)*(to[i]+ta)*(to[i]+ta))-
(ta*ta*ta*ta)))))/(((3*k*t*w)/(4*1))+((h*w*dx)/(cosb)));

delta[i]=fabs((tn[i]-to[i])/tn[i]);
to[i]=tn[i];
}

else if(i==n)
{
tn[n] =(tb-ta);
delta[i]=fabs((tn[i]-to[i])/tn[i]);
to[i]=tn[i];
}
else

{
tn[i]=((((to[i+1]+to[i-1])/(dx*dx))+((to[i+1]-to[i-1])/(2*x[i]*dx)))-
(((2*sigma*emis*1)/(k*t*x[i]*cosb))*(((to[i]+ta)*(to[i]+ta)*(to[i]+ta)*(to[i]+
ta))-ta*ta*ta*ta)))))/((2/(dx*dx))+((2*h*1)/(k*t*x[i]*cosb)));

delta[i]=fabs((tn[i]-to[i])/tn[i]);

```

```
to[i]=tn[i];
}}
```

```
big=delta[1];
for(i=2;i<=n;i++)
{
if(delta[i]>big)
```

```
big=delta[i];
}
niter=iter;
```

```
}while(big>eps);
```

```
for(i=1;i<=n;i++)
{
tt[i]=tn[i]+30;
}
```

```
cout<<"x[i]    "<<"tt[i]    "<<endl;
cout<<endl;
```

```
for(i=n;i>=1;i--)
{
```

```
cout<<x[i]<<"    "<<tt[i]<<"    "<<endl;
cout<<endl;
fout<<x[i]<<"    "<<tt[i]<<"    "<<endl;
}
cout<<"NO OF ITER ="<<iter<<endl;
}
```

|